



# **NAVAL POSTGRADUATE SCHOOL**

**MONTEREY, CALIFORNIA**

## **THESIS**

**AN INVESTIGATION OF THE STATIC FORCE BALANCE  
OF A MODEL RAILGUN**

by

Matthew K. Schroeder

June 2007

Thesis Advisor:  
Co-Advisor:

William B. Maier II  
Andres Larraza

**Approved for public release; distribution is unlimited**

THIS PAGE INTENTIONALLY LEFT BLANK

<b>REPORT DOCUMENTATION PAGE</b>			<i>Form Approved OMB No. 0704-0188</i>	
Public reporting burden for this collection of information is estimated to average 1 hour per response, including the time for reviewing instruction, searching existing data sources, gathering and maintaining the data needed, and completing and reviewing the collection of information. Send comments regarding this burden estimate or any other aspect of this collection of information, including suggestions for reducing this burden, to Washington headquarters Services, Directorate for Information Operations and Reports, 1215 Jefferson Davis Highway, Suite 1204, Arlington, VA 22202-4302, and to the Office of Management and Budget, Paperwork Reduction Project (0704-0188) Washington DC 20503.				
<b>1. AGENCY USE ONLY (Leave blank)</b>		<b>2. REPORT DATE</b> June 2007	<b>3. REPORT TYPE AND DATES COVERED</b> Master's Thesis	
<b>4. TITLE AND SUBTITLE</b> An Investigation of the Static Force Balance of a Model Railgun			<b>5. FUNDING NUMBERS</b>	
<b>6. AUTHOR</b> Matthew K. Schroeder				
<b>7. PERFORMING ORGANIZATION NAME(S) AND ADDRESS(ES)</b> Naval Postgraduate School Monterey, CA 93943-5000			<b>8. PERFORMING ORGANIZATION REPORT NUMBER</b>	
<b>9. SPONSORING /MONITORING AGENCY NAME(S) AND ADDRESS(ES)</b> Office of Naval Research			<b>10. SPONSORING/MONITORING AGENCY REPORT NUMBER</b>	
<b>11. SUPPLEMENTARY NOTES</b> The views expressed in this thesis are those of the author and do not reflect the official policy or position of the Department of Defense or the U.S. Government.				
<b>12a. DISTRIBUTION / AVAILABILITY STATEMENT</b> Approved for public release; distribution is unlimited			<b>12b. DISTRIBUTION CODE</b>	
<b>13. ABSTRACT (maximum 200 words)</b> An interesting debate in railgun research circles is the location, magnitude, and cause of recoil forces, equal and opposite to the launched projectile. The various claims do not appear to be supported by direct experimental observation. The goal of this research paper is to develop an experiment to observe the balance of forces in a model railgun in a static state. By mechanically isolating the electrically coupled components of such a model it has been possible to record the reaction force on the rails and compare that force with the theoretical force on a projectile. The research is ongoing but we have observed that the magnitude of the force on the armature is at least seventy times greater than any predicted equal and opposite reaction force on the rails.				
<b>14. SUBJECT TERMS</b> Railgun, recoil, eutectic, liquid metal, reaction forces			<b>15. NUMBER OF PAGES</b> 93	
			<b>16. PRICE CODE</b>	
<b>17. SECURITY CLASSIFICATION OF REPORT</b> Unclassified	<b>18. SECURITY CLASSIFICATION OF THIS PAGE</b> Unclassified	<b>19. SECURITY CLASSIFICATION OF ABSTRACT</b> Unclassified	<b>20. LIMITATION OF ABSTRACT</b> UL	

NSN 7540-01-280-5500

Standard Form 298 (Rev. 2-89)  
Prescribed by ANSI Std. Z39-18

THIS PAGE INTENTIONALLY LEFT BLANK

**Approved for public release; distribution is unlimited**

**AN INVESTIGATION OF THE STATIC FORCE BALANCE OF A MODEL  
RAILGUN**

Matthew K. Schroeder  
Lieutenant, United States Navy  
B.S., University of Illinois, 1998

Submitted in partial fulfillment of the  
requirements for the degree of

**MASTER OF SCIENCE IN APPLIED PHYSICS**

from the

**NAVAL POSTGRADUATE SCHOOL  
June 2007**

Author: Matthew K. Schroeder

Approved by: William B. Maier II  
Thesis Advisor

Andres Larraza  
Co-Advisor

James Luscomb  
Chairman, Department of Graduate School of Engineering and  
Applied Sciences

THIS PAGE INTENTIONALLY LEFT BLANK

## **ABSTRACT**

An interesting debate in railgun research circles is the location, magnitude, and cause of recoil forces, equal and opposite to the launched projectile. The various claims do not appear to be supported by direct experimental observation. The goal of this research paper is to develop an experiment to observe the balance of forces in a model railgun in a static state. By mechanically isolating the electrically coupled components of such a model it has been possible to record the reaction force on the rails and compare that force with the theoretical force on a projectile. The research is ongoing but we have observed that the magnitude of the force on the armature is at least seventy times greater than any predicted equal and opposite reaction force on the rails.

THIS PAGE INTENTIONALLY LEFT BLANK



# TABLE OF CONTENTS

<b>I.</b>	<b>INTRODUCTION AND MOTIVATION.....</b>	<b>1</b>
<b>A.</b>	<b>INTRODUCTION.....</b>	<b>1</b>
<b>B.</b>	<b>BACKGROUND.....</b>	<b>3</b>
<b>II.</b>	<b>EXPERIMENTAL DESIGN.....</b>	<b>9</b>
<b>A.</b>	<b>KEY DESIGN CONSIDERATIONS.....</b>	<b>9</b>
1.	Sensor Selection.....	9
2.	Power Supply and Rail Material Selection.....	11
3.	Power Coupling.....	11
4.	Testing the Liquid Contact.....	13
5.	Alternative Geometries.....	20
a.	<i>Thin Slots</i> .....	21
b.	<i>Wide Slots</i> .....	25
c.	<i>“T” Bars and “L” Bars</i> .....	27
6.	“Floating” the Rails.....	31
<b>B.</b>	<b>THE PENDULUM SYSTEM.....</b>	<b>32</b>
<b>C.</b>	<b>THE SWITCH.....</b>	<b>36</b>
<b>D.</b>	<b>SYSTEM INTEGRATION.....</b>	<b>38</b>
<b>E.</b>	<b>SENSOR INTEGRATION.....</b>	<b>40</b>
<b>III.</b>	<b>EXPERIMENTATION.....</b>	<b>45</b>
<b>A.</b>	<b>EXPERIMENTAL GOALS AND EARLY TRIALS.....</b>	<b>45</b>
1.	Testing the Design.....	45
2.	Results of the Initial Test.....	49
<b>B.</b>	<b>CAPTURING THE LORENTZ FORCE.....</b>	<b>50</b>
<b>C.</b>	<b>EXPLORING RECOIL VIA ARMATURE REDESIGN.....</b>	<b>56</b>
<b>D.</b>	<b>CONTINUING ARMATURE (RECOIL) TRIALS WITH AND WITHOUT THE COPPER SEGMENT.....</b>	<b>60</b>
1.	Further Tests with the Copper Segment.....	61
2.	Further Tests without the Copper Segment (All-Liquid Armatures).....	64
<b>IV.</b>	<b>DISCUSSION.....</b>	<b>65</b>
	<b>BIBLIOGRAPHY.....</b>	<b>67</b>
	<b>INITIAL DISTRIBUTION LIST.....</b>	<b>71</b>

THIS PAGE INTENTIONALLY LEFT BLANK

## LIST OF FIGURES

Figure 1.	A wire with a perpendicular bend will have an increasingly strong moment to straighten with an increasing magnitude of applied current, if, however, the two sections of the wire are not mechanically coupled (or are loosely coupled) they will be forced apart .....	3
Figure 2.	Two wires of diameter “R” are separated by a distance “W” with a conductive object (armature) between them. If the wires are fixed the armature will experience a Lorentz Force proportional to the applied current squared (that is to say, the applied current down each wire).....	5
Figure 3.	In Kerrisk’s method (similar to my model’s orientation) the width and separation of the rails are in the lateral dimension, while the height is in the vertical dimension. This aspect is that of the breech or bore looking down the longitudinal span of the rails. ....	6
Figure 4.	Here you see the polycarbonate cylinder emptied of the eutectic and the copper bolts only partially threaded. Because we were uncertain of the behavior of the fluid under heavy current loading these early tests employed a nylon-bolted polycarbonate cap. ....	14
Figure 5.	In this simple circuit diagram two 950 CCA batteries are passed through a variable resistor (R1) to limit the current applied to the model railgun (R2). As R1 heated up we needed an alternative means for recording the current applied to the model gun, so we inserted a thermally stable resistance of a known value and placed a voltmeter across the resistor. For additional protection in these early trials we inserted an equivalent 1kA fuse.....	15
Figure 6.	To vary resistance in the circuit we used a device that could compress up to one hundred one-half centimeter thick graphite plates between two copper plates. The copper plates had threaded bolts attached to them for cable connection. By varying the number of carbon plates between the two copper plates and by varying the compressive force squeezing together the plates we could vary the resistance on the order of hundredths of milliohms and still have a fairly large cross-sectional area to disperse power without an extreme temperature rise.....	16
Figure 7.	Towards the center of the figure you can see sooty residue on the polycarbonate threads, this is where arcing was evident during the experiments.....	17
Figure 8.	Here a polycarbonate cap is resting on the polycarbonate cylinder wall. During the experiment the cap was tapped into position with a rubber mallet and the depth of the rounded copper rod was adjusted with a set screw (not pictured). ....	18
Figure 9.	This is a profile view of the polycarbonate cylinder filled with the eutectic and the wetted copper rod. By swapping the terminals we were able to observe consistent fluid behavior regardless of the direction of the current flow. ....	19

Figure 10.	The power supply-bars were fixed with epoxy while the gun-end was loosely constrained by wider slots in a second piece of polycarbonate. With this design we could vary the separation of the electrodes by varying the distance between the notch and the end of the bar. Here you can see two examples of different notch-to-end separation and how these notches were centered on the end-cap.....	20
Figure 11.	The notch in the bar was centered over the end-cap of the eutectic pool. By varying the position of the notch relative to the end of the bar we could vary the power-bar to gun-bar separation .....	22
Figure 12.	In one of the early tests we wanted to ensure that power-end and the gun-end would not repel one another and spill the rather costly eutectic so we employed cable ties to hold the system together. ....	22
Figure 13.	The circuit was quite simple – a pair of car batteries (not pictured) was tied in parallel and the positive terminal was connected to our variable resistor. Current then passed through the resistor into the model gun, through a volt-meter with a known resistance, into a kilo-amp fuse, and to the negative battery terminal. Also pictured (behind the variable resistor) is the micro-ohm meter we used to initially set the variable resistance to limit the applied current. ....	24
Figure 14.	This was one of our wide slots. The right side of the picture depicts the power-end of the model which was connected to the batteries, the triangular cut was the eutectic pool, and the notched bar (left) was the gun-end.....	26
Figure 15.	Unfortunately by the time we thought to photograph the “T” bar and “L” bar designs we had already modified the eutectic pool that the “T” bar was tested in. These are the actual “T” bars we used but the eutectic pool has already been modified to accommodate the larger “L” bars. In the original “T” bar test the bars had a uniform one-half centimeter of eutectic pool on all sides.....	28
Figure 16.	The “L” bar test exhibited significant asymmetrical current flow and was not nearly as successful as the “T” bar design.....	30
Figure 17.	The subtle change here is the removal of the 1kA equivalent fuse. This allowed us to progressively increase the current to a maximum value of 3400A.....	30
Figure 18.	The pendulum system consisted of a series of 5 PVC rail supports suspended by monofilament line. In profile the monofilament was oriented at 90° to the rails, “looking down the barrel of the gun” (i.e. the axial view) you see a small angular deflection (17°) laterally. This deflection greatly enhanced the stability of the system. ....	33
Figure 19.	A photo of the PVC rail supports. Near the center of the frame is the threaded nylon bolt and you can just barely discern a hole in the bolt through which the monofilament line is threaded. You can also see a small section of the copper rail that is fit into one of the slots in the PVC rail support. ....	35

Figure 20.	The aspect shown here is the chamfered edge of the rail support looking up at the all-thread rod where the monofilament line is squeezed between the two nuts. The advantage of this system allowed for continuous “tweaking” of the pendulum as we sought to have consistent tension on all lines and a square and level presentation of the rails to the eutectic and the load cells. ....	36
Figure 21.	This is an operator’s view of the switch – the toggle (1) is centered at the bottom, the pneumatic feed line is on the left, the pneumatic cylinder (2) is on the right, and the upper portion of the 50k Amp switch is attached to the rod coming from the pneumatic device.....	37
Figure 22.	In this view you can see the bus bar (1) from the batteries and variable resistor (upper left) feeding into the top of the mechanical switch (2) via four cables and you can see the large cylindrical switch (3) mounted to the copper bus bar with the eutectic pool mounted to it (4). Also make note of the corners of the lower platform that the switch is mounted on. These “wheel knobs” (5) allowed us to fine-tune the vertical position of the switch (to match the eutectic pool to the lower rail tabs). ....	38
Figure 23.	The two rails labeled “A” and “B” were positioned just above the eutectic pools and the fine-tune adjustments on the switch carriage allowed us to raise the eutectic pools to make contact with the copper tabs hanging down from the rails. ....	39
Figure 24.	This is the road map of the current path from our batteries through the switching and power coupling network to the rails and back into the batteries. ....	40
Figure 25.	This picture shows how we recorded the temperature of the eutectic with a thermocouple and calibrated the infrared camera by adjusting the emissivity setting until the temperature shown on the camera matched the temperature on the thermocouple.....	41
Figure 26.	This photograph shows how we positioned many of the sensors in this experiment. Going clockwise from our technician on the infra red camera we have the IR camera on a tripod (1), the thermocouple meter (2), micro-strain meter and the load cell on the table (3), the high speed camera on a second tripod (4), the high definition camera on the short tripod (5), the micro-ohm meter on the table (6), and the fluke meter on the battery cart (7). Not pictured are three other load cells, an oscilloscope, and a digital camera for still photos. (The “yellow box” is not part of the experiment – just an out-of-control power cord).....	42
Figure 27.	Here you can see the micro-adjustment mount positioned to record the Lorentz force on the pendulum system. The load cell is as close as possible to the arm extending from the rail support without registering a force. In later tests we raised the rails to a height that would allow the load cell to be positioned on the center of the rail support (with no “lever arm” coming off of the support). ....	44
Figure 28.	The center segment of the armature was cut to match the rail separation (5.5 cm) and the upper and lower segments were cut to maximum lateral	

	dimension (11.0 cm). The segments were then coated in Conducto-Lube (an organic based silver-paste electrically conductive lubricant) before being bolted together.....	46
Figure 29.	In the assembled armature the torque applied to the bolts varied the ease by which the armature moved along the rails. While we did not record the torque applied, qualitatively, when it was as tight as we could get it (with an eight inch wrench) the armature was effectively fixed in position. ....	47
Figure 30.	An example of the thermal images we were able to capture during the course of the trial experiment - here you can see calibrated temperature of the fluid and the copper bus bar at 3,800A after 3 seconds. The software processing indicated that the temperature of the fluid was at a maximum of 83°F (28°C) or about 13°F (6°C) above ambient. ....	50
Figure 31.	While it may have been beneficial to examine the data set across a wider spectrum of applied currents and a greater number of trials this early series was conducted simply to determine if the system conformed to the Lorentz force equation, where an increase in force goes as $I^2$ . ....	52
Figure 32.	A log-log plot presents an easy visual reference for comparing the experimental data to the $I^2$ force dependence. ....	53
Figure 33.	In this simple schematic of the pendulum system you can see how the #1 load cell was fixed in position and zeroed and then the #2 load cell (also zeroed) pushed against the pendulum system. ....	54
Figure 34.	Here you see the polycarbonate pool with a copper bar stock segment centered laterally and the eutectic filling the voids to either side of the segment. Also pictured is the very top of micro-adjustment device (for raising the eutectic pool) and the newly attached copper tabs on the underside of the rail ends. In the first such arrangement the bar stock was 4.75 cm in width in a later trial it was trimmed to 4.25 cm in width (pictured here).....	57
Figure 35.	With less than 2 seconds of applied current the arcing between the copper segment and the rail tabs (through the eutectic) deposited a fair amount of the eutectic on the rim of the polycarbonate vessel. This is also a better view of our vertical position micro-adjustor.....	59

## LIST OF TABLES

Table 1.	The data collected from this initial system test was done to determine if we could accurately record the Lorentz force acting on the armature. The single data point for the oscilloscope was collected as a “back-up” if the meter (LED) output was variable or unreadable. After the first trial it was evident that the meter was a reliable output. Every 174 “units” on the force meter represented 100 grams-force, thus the meter value divided by 174 and multiplied by 100 converted “units” on the LED to grams-force. This calibration was achieved by using a variety of known loads on the load cells and realizing a linear relationship.....	51
Table 2.	The table compares the Lorentz Force recorded at the load cell (experimental data) with the Lorentz force calculated using the L’ from Kerrisk. Using the experimental rail-armature Lorentz force and the applied current, I was able to back-calculate a value for “K” describing the electromagnetic character of our system.....	55
Table 3.	This table includes all data to date and additional data points form the section entitled “further tests.” Until approximately 1200A there was no arcing at the bore eutectic pool. After approximately 2200A there was some deflection registered on the force meters. However this deflection was “pulsed” indicating a bounce or possible deflection due to fluid motion. The final 2 trials were conducted with a liquid armature, and in each of these trials there was a smaller deflection.....	63

THIS PAGE INTENTIONALLY LEFT BLANK



## ACKNOWLEDGMENTS

Without the concerted efforts of my outstanding team of lab technicians and peers in the basement of Spanagel Hall this paper never would have seen the light of day. I have the deepest possible appreciation for Don Snyder whom machined those items that were beyond my capabilities, allowed me to tap into over 40 years of electrical and mechanical experience, taught me that modeling on the computer was sometimes more painful than modeling with a band saw, and generally superseded any and all expectations for what a student might expect from a staff member. Not to be outdone by Mr. Snyder, Gene Morris was also instrumental in this process as the lab's jack of all trades. Mr. Morris was responsible for deciphering many cryptic technical manuals on his way to making "things" work like they were advertised, he managed all of my sensor apparatus, recorded all of the data that I neglected to, photographed everything imaginable, and made certain that smooth jazz was always on hand to keep us calm, cool and collected.

Outside of the lab, I must also recognize the incredible support that Professor Bill Maier provided. He recruited me to this project, unknowingly, when he offered assistance in a rather difficult course early in my studies here at NPS. From that moment on I have been his biggest supporter, and from my perspective, he has been mine. When I brought him cost breakdowns and alternatives, Bill would often simply ask me what I needed and trust me to make the right decision – his trust in me bred enthusiasm. I honestly believe that his endless encouragement and advice was the only reason I stayed motivated in over two years of working to try and answer one simple question.

Also, I cannot forget the assistance of Professor Andres Larraza for the ideas that helped to kick start my project and for his assistance in the 11<sup>th</sup> hour as my co-advisor.

Finally, I must acknowledge the financial support of Elizabeth D'Andrea at the Office of Naval Research, without whom this would be yet another theoretical discussion with no experimental results.

THIS PAGE INTENTIONALLY LEFT BLANK

## EXECUTIVE SUMMARY

In more than 20 published papers relevant to railgun recoil, there is much speculation and theory but little or no experimental evidence. According to Newton's third law, when a projectile is accelerated a reaction force must exist, but that force is not necessarily restricted to a reaction on the rails. In this thesis I sought to discover where this reaction force occurs by mechanically decoupling the rails from the power supply and the armature from the rails and then measuring the force on each component.

The magnitude of the force accelerating an armature in an electromagnetic railgun is widely accepted to be  $F = \frac{1}{2} L' I^2$ . This force is a static force and must be transmitted as a reaction to the rails or power source.

By suspending a model railgun as a pendulum and mechanically decoupling the power supply from the rails via a liquid metal contact we were able to precisely record the force on a mechanically coupled rail-and-armature system with a known current. We then decoupled the rails from the power supply and the armature, fixed the armature to the table, and precisely recorded the reaction force.

With current at 2200A in our model gun the theoretical force on the armature (using Kerrisk's  $L'$  of  $0.895\mu\text{H/m}$ ) was 2.16N yet the reaction force on the rails was less than we could measure (with sensitivities as low as 0.024N). Thus, the magnitude of the theoretical force on the armature was at least two orders of magnitude greater than the recoil.

When the armature was tied solidly to the rails, the force on the rail-armature assembly was measured to be of the form  $F = \frac{1}{2} K I^2$ , with  $K \approx 0.33\mu\text{H/m}$ , for  $400\text{A} \leq I \leq 2300\text{A}$ . At  $I=2200\text{A}$ , this force was measured at 1.57N.

At higher currents there was some detection of rail motion but it was at least 70 times less than the force on the rail-and-armature assembly and was most likely due to erratic behavior of the liquid metal contacts (splattering).

While the research is ongoing the results from this series of experiments was quite compelling. The force on the rail-and-armature was observed to be at least 70 times that of any observed reaction force. This led me to the conclusion that there is no perceptible reaction force on the rails in a static condition.

# **I. INTRODUCTION AND MOTIVATION**

## **A. INTRODUCTION**

Over the last thirty-plus years, interest in magnetic accelerator guns (MAGs) such as the electromagnetic railgun has grown considerably. Applications that have been envisioned include everything from replacing the antiquated steam system for rapidly accelerating carrier-based aircraft, to launching orbital platforms, welding or coating surfaces, acting as fuel pellet injectors for nuclear fusion, and firing hypervelocity projectiles as weapons. While many of these applications seem viable from a physics standpoint, the problem of translating concept into design has been riddled with numerous challenges.

In the 1980s, many millions of dollars poured into developing this technology as the Department of Defense was engaged in the Strategic Defense Initiative (SDI) projects. The SDI railgun, called the Compact High Energy Capacitor Module Advanced Technology Experiment (CHECMATE) was developing a means for engaging ballistic missiles from a land-based gun. In the 1990s, the sense of urgency for supporting the research that would foster more technologically mature railguns seemed to wane with the end of the Cold War. Recently, however, the weapons application has come back into focus as the United States Navy has begun progressing towards a new generation of all-electric warships.

The theory that is the basis for any railgun is conceptually simple – to accelerate an electrically conductive armature you need to place it perpendicular to and electrically coupled with another current path such that induced opposing magnetic fields push the objects apart. The advantages, conceptually, that this technology brings to a weapons system include very fast theoretical velocities, propellant-free guns, projectiles at far less cost per shot, less magazine space, and the ability to utilize prime mover power supplies (electric power for tanks or ships) parasitically rather than being powered through chemical gas expansions.

As the Navy has financially expanded its commitment to the maturation of railguns, many different labs are finding themselves in a position to positively influence the ultimate goal of fielding tens of mega-joules guns capable of delivering repeated fire in excess of two thousand meters per second at ranges exceeding two hundred nautical miles. The lab at the Naval Postgraduate School (NPS) is one of these labs.

The railgun lab here at NPS has found its niche in the larger Navy railgun team by chasing after innovative ideas, attempting to resolve theoretical disputes experimentally, and by concentrating interdisciplinary skill sets on complex design and engineering obstacles.

My own thesis work is based around resolving one of those theoretical disputes. What I set out to accomplish was to provide experimental evidence that might help to answer a fundamental physics question: “do railguns recoil?” Railgun theory suggests that one should be able to build a recoilless gun, but, it is impossible to accelerate something with a tremendous amount of force and not pay the price of Newton’s third law.

There are numerous papers (see bibliography) discussing the mechanism for a reaction to the acceleration of the projectile and how one might model this phenomenon. The generalized arguments invoke the Ampere force law or the Biot-Savart law to profess that recoil will be felt throughout a closed circuit (wherever the circuit is closed) (Weldon) or that recoil will be only felt in the breech (Kathe), but there are also papers which claim that railguns may be fired without a breech (Loffler). Some claim

(Allen) that there may be radiation pressure pulses which account for breech recoil or that there are relativistic recoil effects. Others (Graneau) suggest that recoil manifests itself at the rail-armature interface and that these forces can buckle the rails. Still others look at the moving armature (and its induced current) for momentum transfer to the electric field. And some papers have examined the longitudinal electrodynamic forces (along the current path) which can stretch, pinch, or compress materials to conserve momentum (Johansson).

Whatever the case may be, there seems to be a great deal of conjecture but very little experimental evidence to support any of these claims. So, as we began to develop a series of tests to try explore this matter further we approached it as a “win-win” scenario. If the electromagnetic process does not contribute to recoil then this knowledge is an extremely valuable attribute of this type of weapons system. On the other hand, if recoil is evident then we have an opportunity to further refine the governing theory and attempt to determine the basis and magnitude of this force. Before I go into too much detail with respect to my experimental set-up I’d like to first take a bit more time to discuss the theoretical basis of railgun technology.

## B. BACKGROUND

As I stated earlier, the concept of a railgun is quite simple. Through the proper selection of materials and geometry you are able to dictate perpendicular current paths. The flow of current through perpendicular paths induces opposing magnetic fields (in accordance with the “right-hand-rule”). If the perpendicular paths are electrically but not mechanically coupled, the media supporting the current will be forced apart (Figure 1).

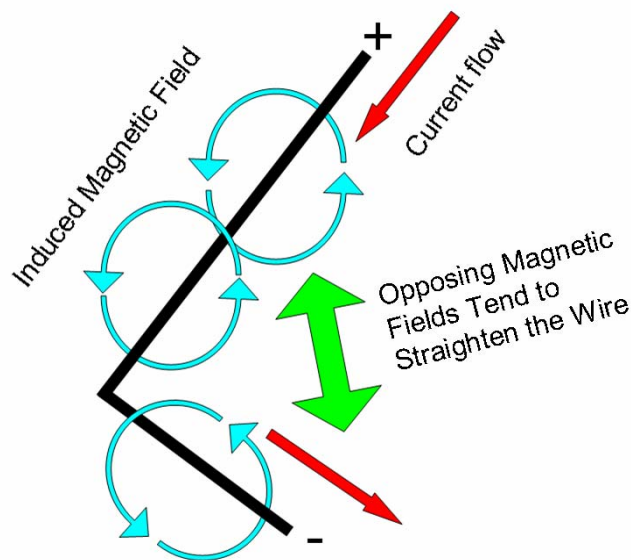


Figure 1. A wire with a perpendicular bend will have an increasingly strong moment to straighten with an increasing magnitude of applied current, if, however, the two sections of the wire are not mechanically coupled (or are loosely coupled) they will be forced apart

The Lorentz force is given by:

$$F = q(E + v \times B) \quad (1)$$

Here,  $F$  is the force on the conductive media in newtons,  $q$  is the coulomb charge of the particle,  $E$  is the electric field as volts per meter, and  $v \times B$  is the vector cross product of media (particle) velocity in meters per second with the magnetic field in teslas.

By applying this expression to a model of two long rods and a spherical armature between them (Figure 2) the Lorentz force becomes approximately:

$$F = ma \approx \frac{\mu_0 I^2}{2\pi} \ln\left(1 + \frac{w}{R}\right) \approx \frac{L' I^2}{2} \quad (2)$$

This expression for the Lorentz force, one-half of the “Inductive Gradient” multiplied by the square of the current, is a widely accepted theoretical form of the force provided by conducting rails on an accelerating armature (Maier).



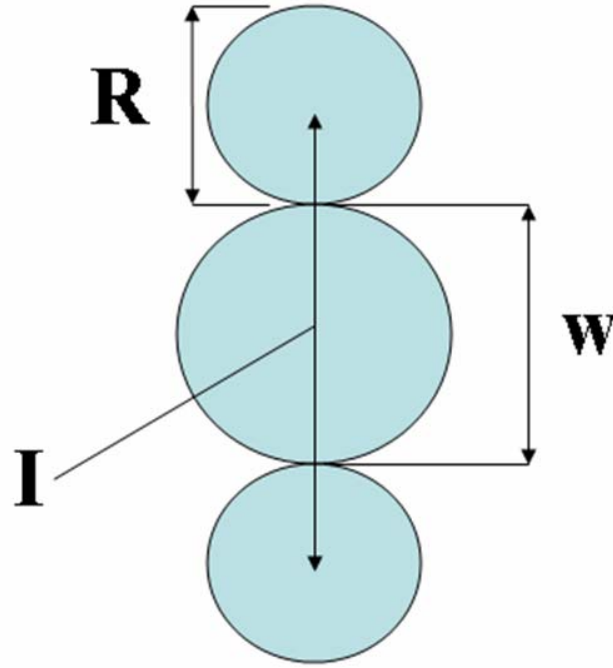


Figure 2. Two wires of diameter “R” are separated by a distance “W” with a conductive object (armature) between them. If the wires are fixed the armature will experience a Lorentz Force proportional to the applied current squared (that is to say, the applied current down each wire).

The magnitude of the current,  $I$ , is simply found by Ohm’s Law, while the inductive gradient,  $L'$ , is estimated to be on the order of tenths of micro-Henries per meter ( $10^{-7}$  H/m) for most systems then back-calculated as experimental data (such as velocity) is collected.  $L'$  is proportional to the Lorentz force and it is also dependent upon geometry, and materials. I used Kerrisk’s method (Kerrisk) to calculate an initial estimate of  $L'$  in my experiments. This method, developed at Los Alamos National Laboratory, takes into consideration the geometry of the gun and various material and logarithmic constants (Figure 3).

$$L' = \left[ A + B \ln \left( 1 + a_1 \frac{w}{h} + a_2 \frac{w}{h} \frac{s}{h} \right) \right] \ln \left( b_1 + b_2 \frac{s}{h} + b_3 \frac{s}{h} + b_4 \frac{s}{h} \frac{w}{h} \right) \quad (3)$$

The constants are:

$A=0.440641$   $B=-0.07771$   $a_1=3.397143$   $a_2=-0.06603$

$b_1=1.007719$   $b_2=2.743651$   $b_3=0.022093$   $b_4=0.263739$

The geometric factors are:

$w$ =rail width (mm)     $s$ =rail separation (mm)     $h$ =rail height (mm)

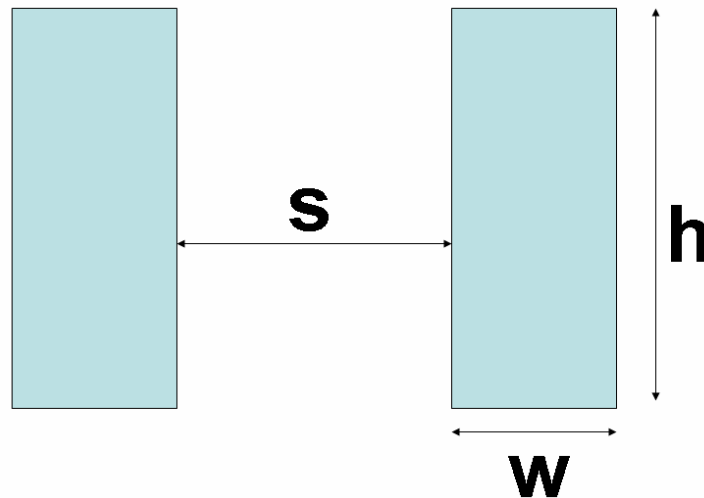


Figure 3. In Kerrisk's method (similar to my model's orientation) the width and separation of the rails are in the lateral dimension, while the height is in the vertical dimension. This aspect is that of the breech or bore looking down the longitudinal span of the rails.

Equation (2) suggests that until materials begin to degrade, the more current you apply to the gun the more force you produce and consequently the more you are able to accelerate a projectile. For practical purposes the resistance in the power supply and the resistance in the power-coupling network are the limiting factors.

As I move on into a discussion of my experimental set-up you will see that even though my experiments were performed on a model that is the conventional “two rails and an armature” description of a railgun, I’ve generalized the theory for this physical system because not all railguns operate in this conventional fashion.

THIS PAGE INTENTIONALLY LEFT BLANK

## **II. EXPERIMENTAL DESIGN**

### **A. KEY DESIGN CONSIDERATIONS**

Since our experimental goal was to try and detect any apparent recoil, it was necessary to design an experiment that isolated a model gun and armature from everything else, that the rails carried sufficient current to exert a detectable electro-magnetic force on the armature (and consequently the rails), and that this force had to be detected in a quasi-static state. We also needed to ensure that the design permitted repeatable tests, that it was conducted in a laboratory-safe environment, that we could complete it in a reasonable amount of time, and that cost was minimized. Yet, since we were doing an truly unique experiment, the most effective process seemed to be an iterative series where we designed a little, tested a little, reviewed, refined, and repeated.

#### **1. Sensor Selection**

The first step in this process was to select a force-detection system that was robust enough to withstand high current and high electro-magnetic pulses, yet affordable and sensitive enough to be definitive. I investigated hydro-pneumatic sensors, bondable-terminal solder-tab strain meters, micro-filament semi-conductor (epoxy) gauges, laser-vibrometers, and high-speed cameras before ultimately selecting piezo-resistive micro-load cells.

Many of these devices had characteristics that were desirable and there might have been useful information gained by using them, but the initial series of tests was simply to determine “if” the rails move. If the answer to that question was an affirmative “yes” then follow-on tests might take advantage of these other sensors’ attributes to detect the magnitude, direction, and cause of the force (more precisely).

Terminal solder-tabs were cheap, sensitive, easily applied and easy to calibrate, but there were concerns about what high current loading would do to the tabs and consequently how we might shield these devices.

Micro-filament semi-conductor gauges were the most sensitive devices but were difficult to apply and calibrate and again might be susceptible to saturation or damage from high current and electro-magnetic pulsing.

Laser-vibrometers and high-speed cameras had the advantage of being electrically isolated from the experiment and very sensitive, but they were rather costly and did not seem well-suited to a quasi-static test where a detectable force was the most desired output (and not simply motion).

The load cells had the ability to be electrically isolated, they were cheap, and they were easy to use and easy to calibrate. The concern on the load cells was the level of sensitivity. We suspected that even the most sensitive compressive load cells would require a minimum of two to three newtons to output a satisfactory reading. Therefore the selection of our detectors had a direct impact on the ultimate design of the model gun and its power supply.

The detectors we selected were miniature industrial compression load cells LCGB-50, LC305-25, and LCGC-150 from Omega Engineering. All gauges had a ten volt direct current excitation with several millivolts of output and could be calibrated to detect force in tenths of a newton at  $\pm 0.10\%$ . The LCGB-50s had a maximum loading of 23kg (50lbs) at a maximum deflection of  $80\mu\text{m}$  (0.003in). The LC305-25s were more sensitive detecting maximum loads of 11kg (25lbs) at maximum deflections of  $2.5\mu\text{m}$  (0.001in). The LCGC-150 was the most sensitive detecting maximum loads of 150g with deflections in the micrometer range, however, this gauge did not arrive in time for inclusion in this paper. All gauges had insulated 1.5m (5ft) AWG30 cables that could be coupled to a wheat-stone bridge or other variable resistance, voltage, or current detector. The pre-calibrated meter we selected was an Omega Engineering DP41-B-4R-A-EI 1/8 DIN ultra-high performance meter with accuracy to 0.005%, 166 samples per second, four isolated collector input/output ports with digital/analog capabilities and Ethernet compatibility. This device offered pre-calibrated resistance, voltage, and current detection that could accept the output range of the load cells (0-100mV), provided internal excitation, and was advertised as having the ability to output gauge readings to various software programs.

## **2. Power Supply and Rail Material Selection**

If the Lorentz force equations I employed are the correct expressions for the force on the armature, then one might expect that recoil would be less than or equal to this force (equations (1) and (2)). Therefore, the next logical step consisted of designing a nominal rail system and power supply that would theoretically produce a force that these detectors could reliably measure and record.

Rail material that was readily available in the lab consisted of 2.5cm by 0.5cm copper bar stock in variable lengths. To preserve the integrity of this experiment I needed to select a bar length such that any current path parallel to the armature would be in the far-field and not directly influenced by the magnetic field of the armature. A conservative estimate was 6ft (1.872m). I also needed to select an arbitrary rail separation for the purposes of calculating an initial inductive gradient. Since the width of the bar stock was 2.5cm I selected my initial rail separation to the same dimension (2.5cm)..

After selecting my rail dimensions and inputting them into Kerrisk's equation (Equation 3) I estimated an  $L'$  of  $0.685\mu\text{H/m}$  for this nominal design. Using this  $L'$  in the Lorentz force equation with variable current applied I found that we could expect approximately 0.3N at 1kA and up to 34N at 10kA. In order to supply several kilo-amperes for a static experiment (for an arbitrarily selected interval of 3 seconds) and to repeat this power application several times in a relatively short duration (a day or less) we determined that automotive batteries were the most likely candidates.

We selected high cold-crank-amp (CCA) automobile batteries capable of producing 1000A at ambient temperature. The battery model I selected was an Autolite 96 Platinum, rated at 950 CCA at  $0^{\circ}\text{C}$ .

## **3. Power Coupling**

Accurately estimating the Lorentz force, building the gun, and selecting the power supply were the simplest parts of this project. Coupling the power supply electrically but not mechanically was probably the most difficult.

Mechanically de-coupling the rails and the power supply was important because it was totally impractical to try and devise a system where we could detect motion of the entire gun in one direction and the armature in the other. With a decoupled power supply we could choose to fix the position of the rails, fix the position of the armature, or allow both to move freely. By mechanically isolating the power supply from the gun and the armature it was possible to focus our attention on whether or not the force pushing the armature down the rails (and the accompanying current and magnetic fields) would result in any apparent recoil (reaction of the rails in the opposite direction).

Several methods were proposed for this mechanical isolation. We researched wire brushes, wetted-wire brushes and bearings before exploring liquid contacts.

Wire brushes are a commonly used means of coupling power supplies to moving objects, however a densely packed brush which can handle high current loading has a correspondingly high amount of friction. Conversely, a loosely packed brush has lower friction but won't permit enough power dissipation for the brushes to handle high current loading. Wetted brushes have both desired characteristics of high current loading and low friction, but were incompatible with this experiment because of the extensive effort required to engineer a fluid containment and recycling apparatus.

The liquid contacts were the most attractive because of the very low friction and assumed ability to handle high current loads. We also believed (early-on) that engineering a system for coupling the rails to the power supply with the liquid was almost as simple as replacing wire leads with liquid channels.

In my initial designs for a liquid contact I explored measuring recoil by hydrodynamic processes. The idea was to confine conductive liquid in a non-conductive cylinder with the end of a rail acting as a piston so that any recoil would result in a displacement of liquid from the cylinder and the force for the displacement could be calculated. While this design seemed to be the easiest it was ultimately rejected because of the (assumed) necessity for a gasket and because we were uncertain how the fluid might react in a confined space under high current.



We instead chose a liquid filled slot as our electrical coupling. This design employed a fixed power supply driving current into a slot filled with liquid metal. I envisioned that the model gun would be suspended as a pendulum with the breech end sliding freely in the liquid filled slots. I would have to correct for the restoring force of the pendulum system, but essentially the free swinging pendulum would provide visual confirmation of “recoil.” To quantify the motion of the pendulum system we would place the various push-button strain gauges (the micro-load cells) in fixed positions around the pendulum system.

The process of selecting a conductive liquid contact was relatively simple. The desired characteristics were a thermally and chemically safe, yet highly conductive material that was readily available. In my research on wetted brushes I had become familiar with an Indium Gallium Eutectic (74.5% Gallium and 25.5% Indium, by weight) that was highly conductive and thermally stable. Although information on material density, conductivity, and thermal properties seemed to vary, eventually we determined that the majority of the data was in an acceptable range. Not much else was known about the liquid. We did not have a good understanding for how it might function in a high current and magnetic field, what materials it would wet, how viscous the fluid was in an assumed operating temperature, and many other considerations. So, to design a system that would perform the types of operations we needed, it was imperative to begin testing the liquid in many conceivable orientations.

#### **4. Testing the Liquid Contact**

Our first experiment was a simple test to determine qualitatively what the liquid would do under high current. I threaded two copper bolts into a machined polycarbonate vessel oriented at ninety degrees, sealed the openings with silicone, filled the vessel with the eutectic, and capped it with a sheet of polycarbonate (Figure 4). I then set up a current limiting circuit of  $15\text{m}\Omega$  (Figures 5 and 6), put a voltmeter in parallel, and connected it with two 12V car batteries in parallel. The current was effectively limited to 800A. I then connected the current limited circuit to the bolts threaded into the eutectic for a period of approximately 5s. The liquid showed considerable deflection with arcing

evident on the bolt threads. After repeated tests of 3-5s there was evidence of oxidation near the copper electrodes and burn marks on the polycarbonate near the copper penetration (Figure 7). With the apparent symmetry of the experimental design there was purpose in reversing current flow. The fluid itself had no qualitative indication of having changed its material properties. In other words it “looked the same” as it did prior to the series of tests. Subsequent weight measurements of the eutectic offered nothing to contradict this claim.

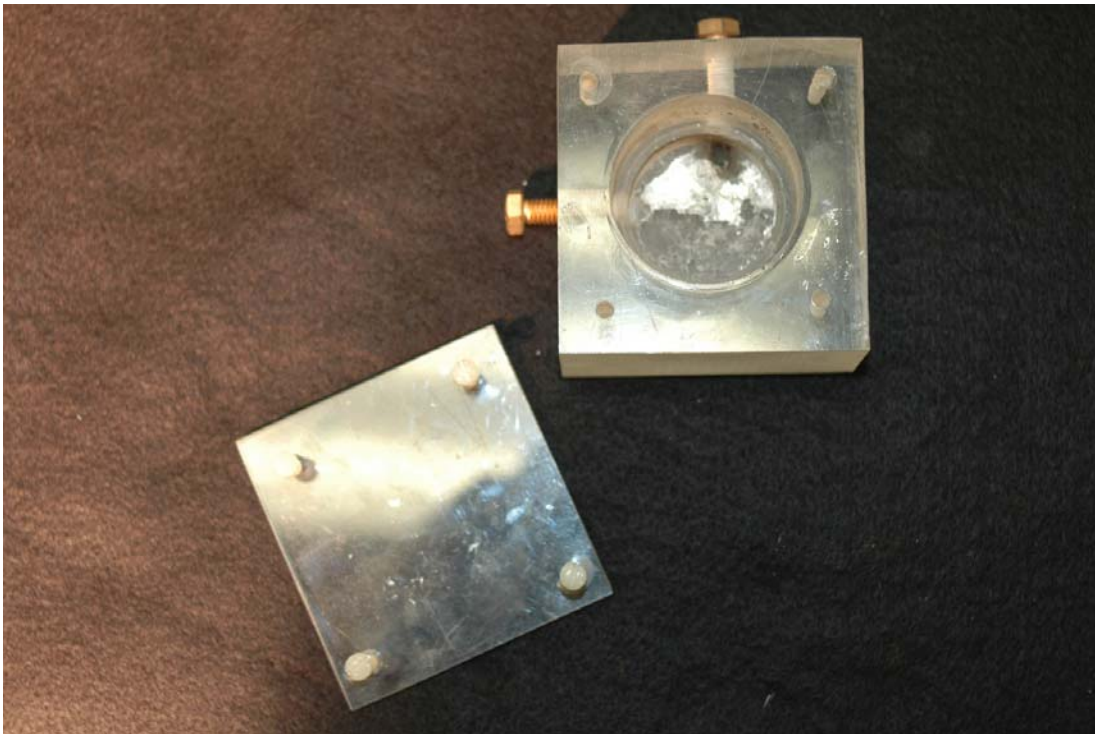


Figure 4. Here you see the polycarbonate cylinder emptied of the eutectic and the copper bolts only partially threaded. Because we were uncertain of the behavior of the fluid under heavy current loading these early tests employed a nylon-bolted polycarbonate cap.

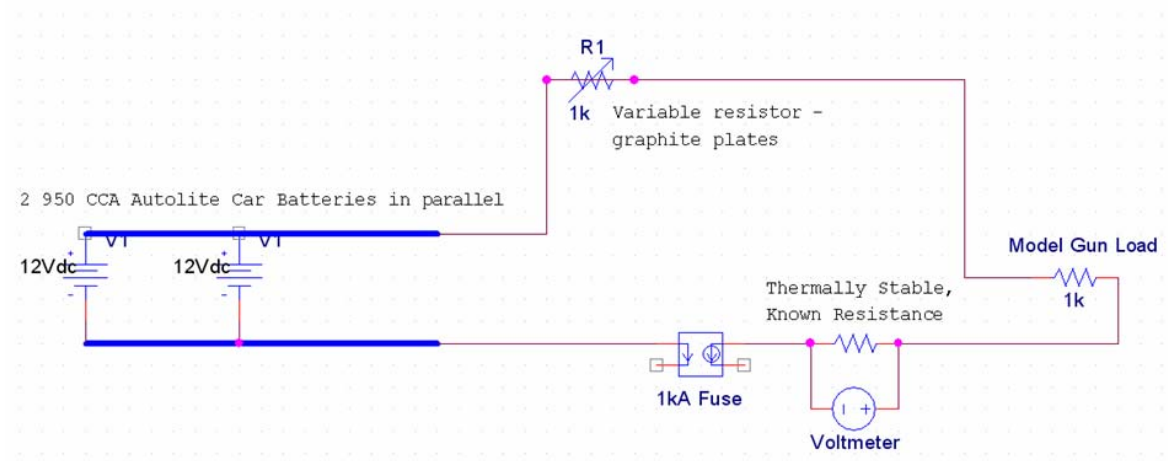


Figure 5. In this simple circuit diagram two 950 CCA batteries are passed through a variable resistor (R1) to limit the current applied to the model railgun (R2). As R1 heated up we needed an alternative means for recording the current applied to the model gun, so we inserted a thermally stable resistance of a known value and placed a voltmeter across the resistor. For additional protection in these early trials we inserted an equivalent 1kA fuse.

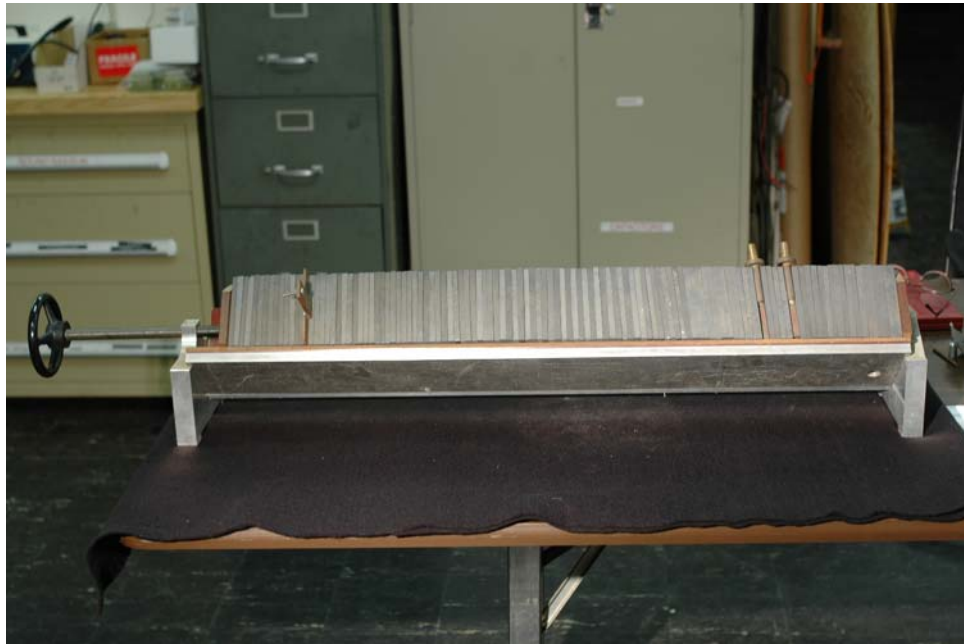


Figure 6. To vary resistance in the circuit we used a device that could compress up to one hundred one-half centimeter thick graphite plates between two copper plates. The copper plates had threaded bolts attached to them for cable connection. By varying the number of carbon plates between the two copper plates and by varying the compressive force squeezing together the plates we could vary the resistance on the order of hundredths of milliohms and still have a fairly large cross-sectional area to disperse power without an extreme temperature rise.

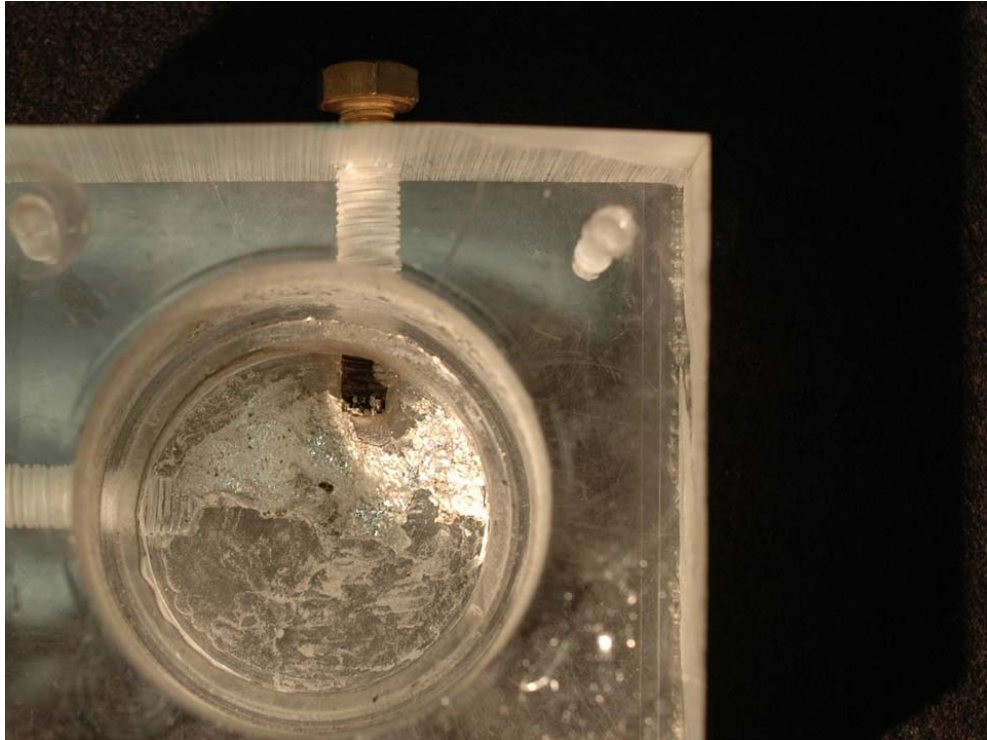


Figure 7. Towards the center of the figure you can see sooty residue on the polycarbonate threads, this is where arcing was evident during the experiments.

By studying the video recordings of these early tests I came to suspect that the arcing was probably due to the threads of the bolts being wetted by the eutectic. Furthermore it seemed that the arcing was probably the main contributor to the deflection of the fluid (either by thermal or electro-magnetic action). For a second trial I opted to present only smooth surfaces arranged in the most symmetric orientation (Figure 8).

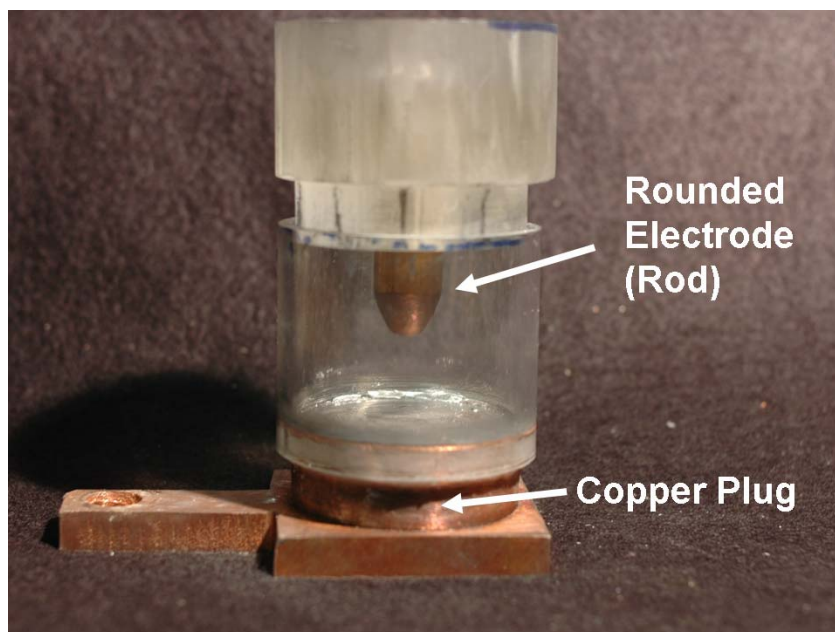


Figure 8. Here a polycarbonate cap is resting on the polycarbonate cylinder wall. During the experiment the cap was tapped into position with a rubber mallet and the depth of the rounded copper rod was adjusted with a set screw (not pictured).

Using a polycarbonate tube as a vessel for the eutectic, I machined a copper plug for the bottom of the tube (sealed with silicone) and threaded a bolt into the bottom of this plug for electrical connection. One of our lab technicians fabricated a polycarbonate cap for the top of the tube and drilled a hole in it for a copper rod electrode. I then used a belt sander to round the tip of a 0.5in diameter copper rod and threaded the opposite end of the rod for electrical connection. With the copper rod electrode inserted into the hole in the cap a set screw through the cap allowed for different rod-to-plug separation. I then filled the tube with eutectic (recovered from the pervious test). For the initial test of this geometry the rod-to-plug separation was set to 2cm with approximately 1cm of the rod wetted in the eutectic (Figure 9).



Figure 9. This is a profile view of the polycarbonate cylinder filled with the eutectic and the wetted copper rod. By swapping the terminals we were able to observe consistent fluid behavior regardless of the direction of the current flow.

As in the previous test I connected the current limiting circuit across the eutectic (approximately 800A) for 5 seconds. This time the results were very favorable, as there was no action whatsoever on the fluid. Subsequent tests for intervals exceeding 10s seconds had the same result. After five tests of longer time intervals we reversed the leads from the battery supply (reversing the current flow in the eutectic) and still detected no fluid motion. Decreasing the rod-to-plug separation from 2cm to approximately 0.5cm likewise made no discernable change.

In our estimation this series of tests demonstrated that with the right geometry this fluid was acceptable at currents up to 800A. No thermal data were collected due to the inability of the available infrared detectors to collect data through the polycarbonate enclosure. However, future tests were designed to permit temperature measurement to ensure safe working conditions (well below an unsafe vapor pressure of the eutectic).



The next step was to determine what geometries could we use and what was the upper limit to the applied current before the fluid began reacting in an unfavorable manner.

## 5. Alternative Geometries

These next series of tests employed a small-scale model of a railgun. We used the same bar stock (2.5cm by 0.5cm) cut to lengths that would be easy to work with and support on a laboratory table (Figure 10). We then attempted several geometric configurations of rail-to-power supply couplings with the eutectic by varying the shapes and orientations of the contacts, by varying the separation of the contacts, and by varying the amount of liquid.

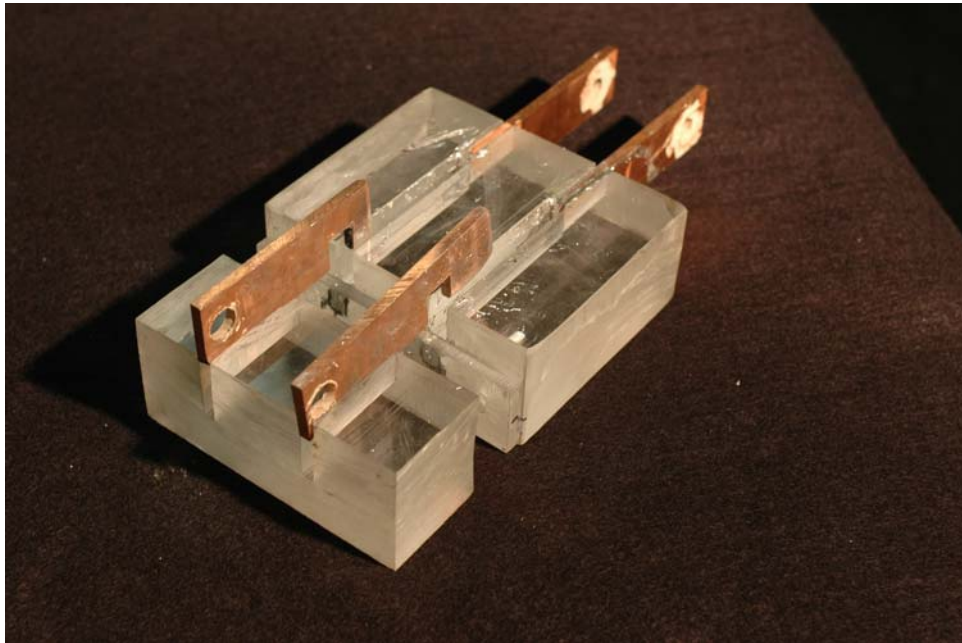


Figure 10. The power supply-bars were fixed with epoxy while the gun-end was loosely constrained by wider slots in a second piece of polycarbonate. With this design we could vary the separation of the electrodes by varying the distance between the notch and the end of the bar. Here you can see two examples of different notch-to-end separation and how these notches were centered on the end-cap.



*a. Thin Slots*

The first series of tests using the small-scale gun was an aggressive departure from the “most-symmetric” design. We cut two channels in a 12cm wide by 10cm long by 5cm high polycarbonate block, filled the channels to some depth of eutectic (approximately 1.5cm), and placed two copper bars in each channel, separated by some distance (the distance varied as the notch-to-end distance was varied). On the power supply-end of the channels the bars were fixed in position with six-minute epoxy (sealing off the end of the channel). On the gun-end of the channels a 12cm wide by 0.5cm long by 3.5cm high end-cap piece of polycarbonate was fixed by epoxy. The rods on this gun-end had a 1.5cm long by 1.5cm high section removed to serve as a notch and 1.5cm diameter holes drilled to serve as bolt-holes (Figure 11). The notched sections of the bar stock were placed over the polycarbonate “end cap.” A 1.5cm diameter by 9cm brass bolt was passed through the bolt holes to couple the gun-end bars together (simulating an armature). The fixed bars then served as a power supply and the notched and bolted bars acted as a free-moving rail and armature system (Figure 12). In an ultimate design the gun-end bars would be significantly longer, the armature would be free moving, and the rails would be supported by a pendulum system that would allow the rails to move freely.



Figure 11. The notch in the bar was centered over the end-cap of the eutectic pool. By varying the position of the notch relative to the end of the bar we could vary the power-bar to gun-bar separation

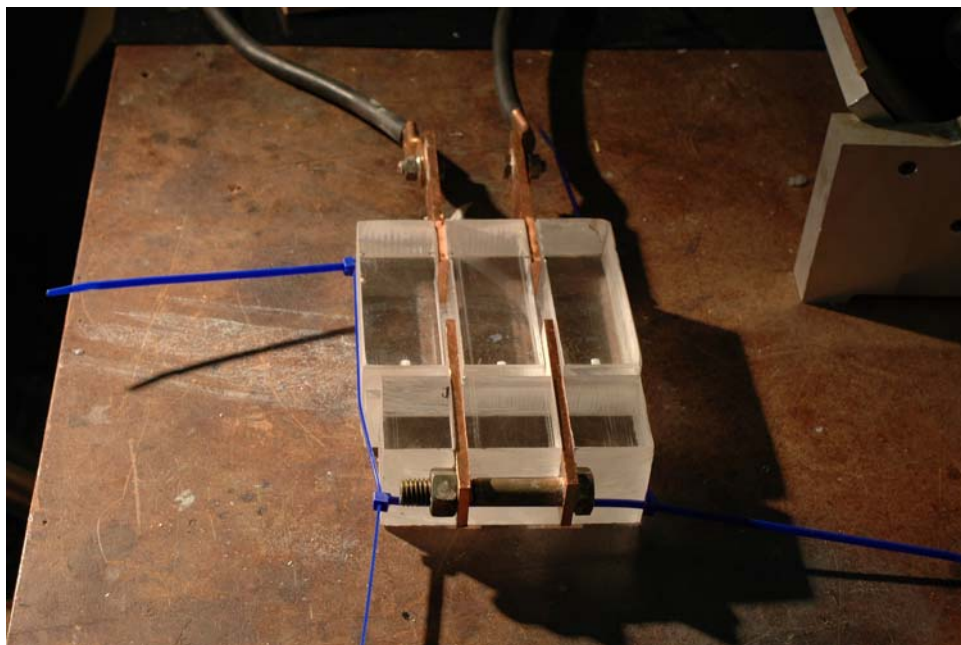


Figure 12. In one of the early tests we wanted to ensure that power-end and the gun-end would not repel one another and spill the rather costly eutectic so we employed cable ties to hold the system together.

With the power coupling assembled we had two 12cm-long copper bars providing electrical contact between parallel car batteries and a channel of eutectic. The cross-sectional area of the bars presented to the eutectic was approximately 0.5cm by 1.5cm ( $0.75\text{cm}^2$ ) per bar with some error in the measure attributed to the eutectic meniscus. The eutectic-only channel (volume where the power-bars and gun-bars were separated) was 1cm wide by 1.5cm high and 1 to 4 cm long ( $1.5\text{cm}^3$ - $6\text{cm}^3$  of fluid). The gun-bars presented a much larger electrical contact area as up to 3cm of the rod was protruding into the liquid channel (the notch setting on the end-cap was 3cm from the end of the bar for the least-separation test). The surface contact area presented to the eutectic from the gun-bars was approximately 3cm long by 1.5cm per side and the 1.5cm by 0.5cm on the end (for a total of  $9.75\text{ cm}^2$ ). Using the variable resistor we once again limited the current to 800A and applied the current to the system for 3s (Figure 13).

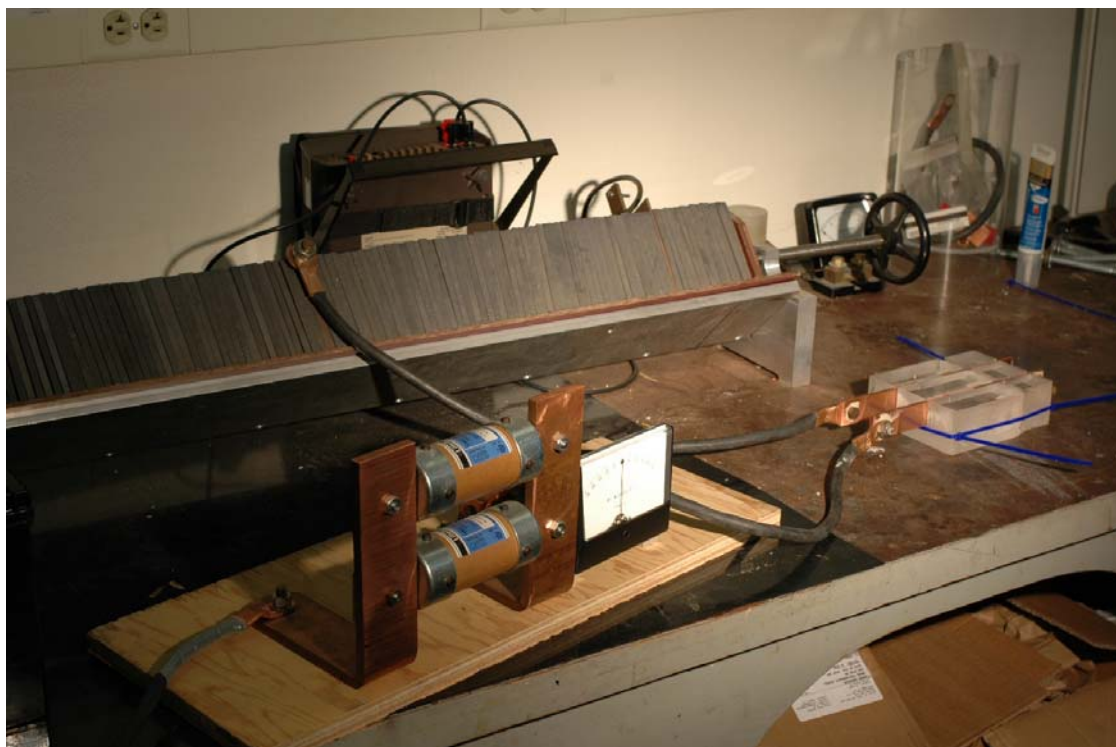


Figure 13. The circuit was quite simple – a pair of car batteries (not pictured) was tied in parallel and the positive terminal was connected to our variable resistor. Current then passed through the resistor into the model gun, through a volt-meter with a known resistance, into a kilo-amp fuse, and to the negative battery terminal. Also pictured (behind the variable resistor) is the micro-ohm meter we used to initially set the variable resistance to limit the applied current.

We observed a small amount of fluid deflection at the power-end of the channel with a significantly greater amount of fluid deflection on the gun-end. There was no apparent splatter of the fluid, but there were rippling waves as far as 1cm from the bar on the gun-end which were as high as 2mm. The viscosity of the fluid damped the wave motion quite rapidly, but the ripples were nevertheless disconcerting. With the presence of waves in the fluid at the gun-end it was going to be more difficult to detect recoil motion reliably. My hypothesis was that with a high enough current we could determine qualitatively that the rails were going to recoil (or not) but any measurement on motion of the rails would be subject to the push and pull of the waves in the fluid. Similar to a large vessel moored securely to a pier, the wave motion is barely perceptible standing on the deck of the vessel, but at the interface of the water and the hull you are very aware of the action.

Subsequent analysis of this geometry on COMSOL Multi-Physics revealed certain problems with the asymmetric current density of the fluid-rail contacts (that we had observed in the experiment). As we gained familiarity with this program it became beneficial to model future designs before we spent valuable time and effort in fabricating systems and performing tests.

#### ***b. Wide Slots***

Based on the information gained from the thin-slot experiment we decided to widen the slot on the gun-end to try and minimize the asymmetry of the current flow and obtain as uniform-as-possible current density into the surface of the copper rail. The notion here was that waves on the rails perpendicular to the direction of the recoil would cancel and the waves in the same (or opposite) direction of the recoil would be less (as the current density on the end of the rail was reduced). We modeled various designs on COMSOL and ultimately chose a design where current density was relatively high at the power-end of the eutectic but dispersed to almost one-tenth of the density at the gun end. This tapered design was chosen over a design, for example, with a channel that was simply ten times as wide due to the scarcity and cost of the eutectic. At numerous

instances throughout this process I declared that if I could afford a “trash-can-sized vat” of this fluid the experiment we would be much easier.

Again we used polycarbonate as the rigid material to contain the fluid. This tapered design consisted of a 0.5cm by 3cm high slot (where the power-bar was fixed by epoxy) that widened to a 7cm slot in a span of 2cm (effectively creating a three-dimensional triangular cut). The 7cm slot extended from the end of the taper to a distance of 3cm further down in the polycarbonate block. At the end of the widened channel a polycarbonate end-cap piece was fixed in place to contain the eutectic pool, as in previous tests. In this 3cm by 7cm span the notched copper bar was centered with the notch over the end-cap (Figure 14).

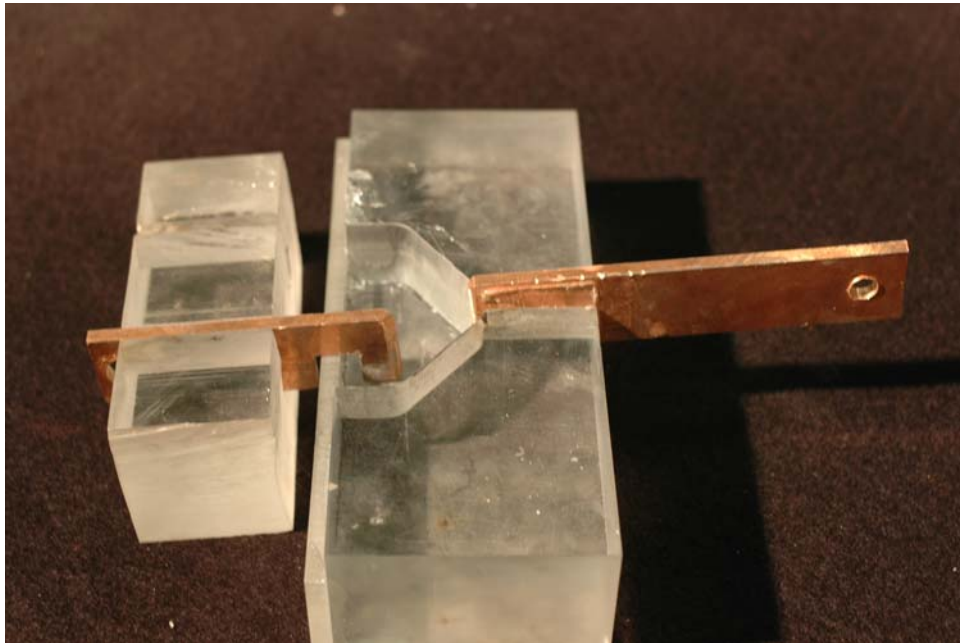


Figure 14. This was one of our wide slots. The right side of the picture depicts the power-end of the model which was connected to the batteries, the triangular cut was the eutectic pool, and the notched bar (left) was the gun-end.

Prior to connecting the power supply to the circuit and delivering the usual 800A, we sought-out a means of developing a temperature rise profile. To collect temperature data on a medium passing high current loads it was important to have an adequately shielded thermo-couple or some sort of infra-red detection system. Readily

available was a thermo-couple and an Agema Thermovision 550 IR Camera. The thermo-couple would not perform under high current loading of the fluid but it was useful for calibrating the emissivity setting of the IR Camera (set to 0.65 of a unit, 1.0, reference from Aluminum). Once we calibrated response it was simply a matter of aiming the camera at the fluid and selecting an appropriate sample rate (100Hz).

When current was applied to the circuit the deflection at the corners was noticeably less than in the previous “narrow slot” test. However, the fluid continued to ripple slightly throughout each of the five to seven second tests. The magnitude of the fluid deflection (ripple) was estimated to be less than one millimeter and there was no evidence of splattering or arcing.

The temperature of the laboratory environment at the time of the experiment was 22°C. Prior to shorting the circuit the temperature of the eutectic was 21.8°C. The average temperature rise in the eutectic over a 5 second span at 800A was well within the safe operating range at 13°C. After 7 seconds at 800A the recorded temperature average (of two trials) was 35°C. These values were significantly less than the anticipated temperature rise, so to confirm the data recorded in the IR camera we measured the temperature rise with the thermocouple once the circuit was opened. While we did not purposefully allow for the eutectic to cool to the ambient condition between subsequent tests, the material shed its thermal energy rapidly. On average, within 10 seconds of opening the circuit the temperature of the eutectic was at ambient temperature.

### *c. “T” Bars and “L” Bars*

By widening the slot we believed we had achieved the goal of reducing the current density of the fluid-copper interface on the gun-end (negative terminal) of the eutectic pool. Evidence of this was a very low temperature rise and a reduction in the fluid ripple. However, as previously stated, the earliest tests – that of the rounded copper rod dipping into cylinder of eutectic – demonstrated that it was possible to design a geometry where there was no detectable fluid deflection whatsoever (up to 800A). So, we began to consider how we might select a geometric configuration that might model this earlier test, yet conform to the slotted-rail design.



We tested both “T” shaped bars and “L” shaped bars (Figures 15 and 16 respectively). In the no-ripple tests we felt that the uniform flow of current eliminated any asymmetrical current density and its subsequent thermal convective flow and/or chaotic magnetic field perturbation. By increasing the cross-sectional area of the copper on both the positive and negative terminals we were imagining a situation not-unlike a parallel-plate capacitor. The first design, the “L” bar, was accomplished by simply putting one end of our bar stock in a large vice and bending it to a ninety-degree angle. Once we bent the bars and began trying to machine-out a eutectic pool in the polycarbonate we realized that “T” bars might be easier to work with. So we cut a 10mm deep by 0.5cm wide slot on the broad side of a scrap piece of our bar stock. We then fitted the end of a copper bar into the slot and filleted the bar in place with solder. Next we trimmed the ends of the scrap copper bar to 1.5cm from the fillet and polished all of the surfaces with wet-dry sand paper (Figure 15).

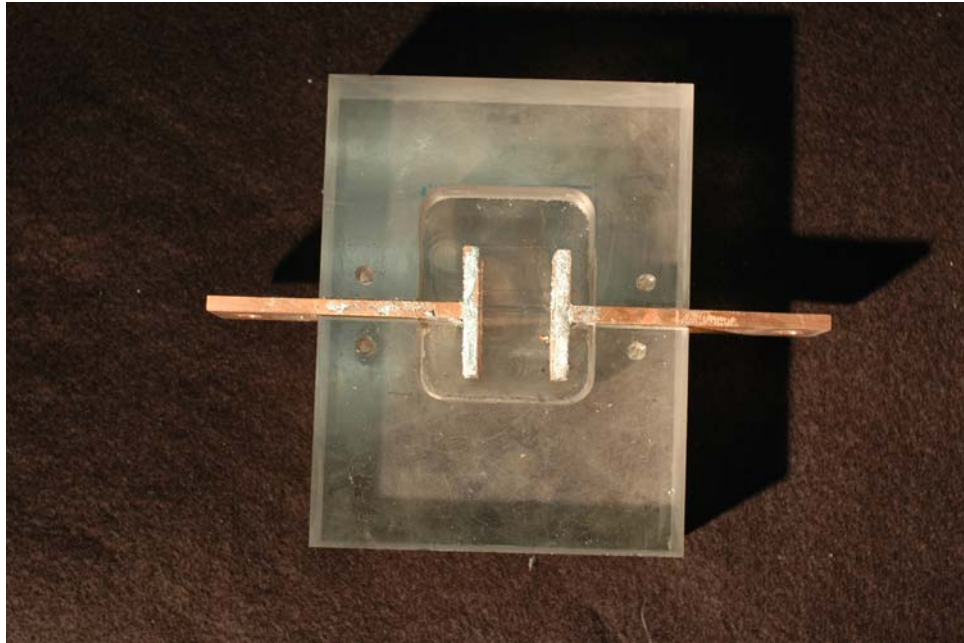


Figure 15. Unfortunately by the time we thought to photograph the “T” bar and “L” bar designs we had already modified the eutectic pool that the “T” bar was tested in. These are the actual “T” bars we used but the eutectic pool has already been modified to accommodate the larger “L” bars. In the original “T” bar test the bars had a uniform one-half centimeter of eutectic pool on all sides.



Once we had the “T” bars made we inserted them into a 4cm long by 4cm wide by 2.5cm deep slotted polycarbonate eutectic pool. Unlike previous tests both bars were fixed in position and there was no notch on either bar. Therefore, we opted to use all available eutectic and fill this pool to its maximum depth of just under 2.5cm.

The eutectic filled pool was connected to the variable resistance circuit in the usual manner and we shorted the circuit at 800A. As in previous tests some fluid ripple was evident, but it was noticeably less than even the wide slot tests. As we varied the separation of the terminals from 1cm to 0.1cm we observed very little change in the fluid’s behavior. So, in an effort to gain more knowledge on the behavior of the fluid we decided to increase the current progressively. In order to accomplish this we utilized a milliohm meter to set the variable resistor and we removed the 1kA fuse (Figure 17).

As we cautiously stepped the current from 800A to 3800A ( $3.6\text{m}\Omega$  at 12.4V) some small increase in fluid ripple was apparent, but the maximum amplitude of the deflected waves was still on the order of 1mm or less. So, we felt confident that this geometric arrangement was a strong candidate for the final power coupling design.

The “L” bar test was conducted at the usual 800A in the same pool as the “T” bar test with a slight modification in one dimension of the pool (increasing one side from 4cm to 6cm in length, Figure 16). The pool was filled to its maximum depth of approximately 2.5cm. Fluid ripple was slightly more pronounced around the region where the bars were bent.

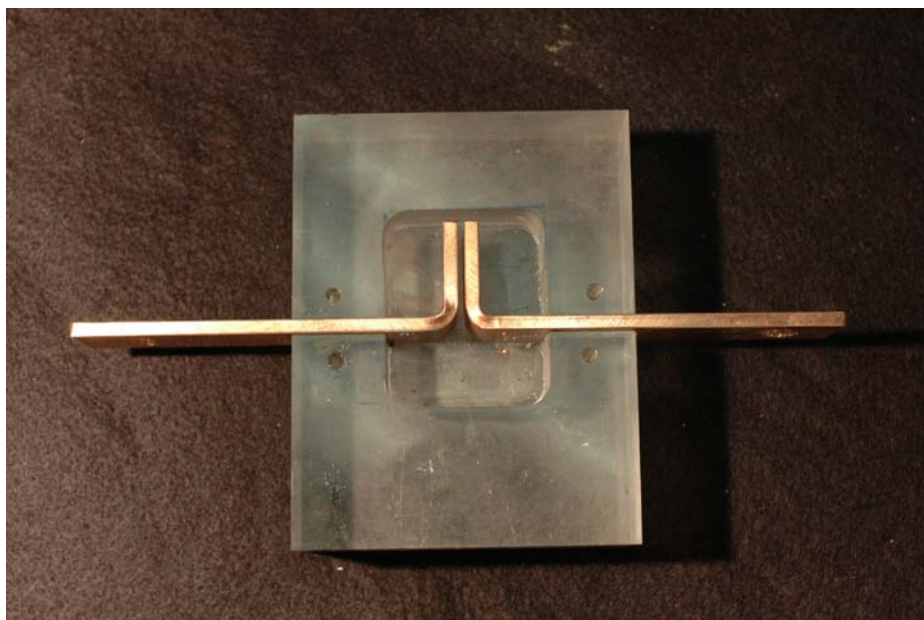


Figure 16. The “L” bar test exhibited significant asymmetrical current flow and was not nearly as successful as the “T” bar design.

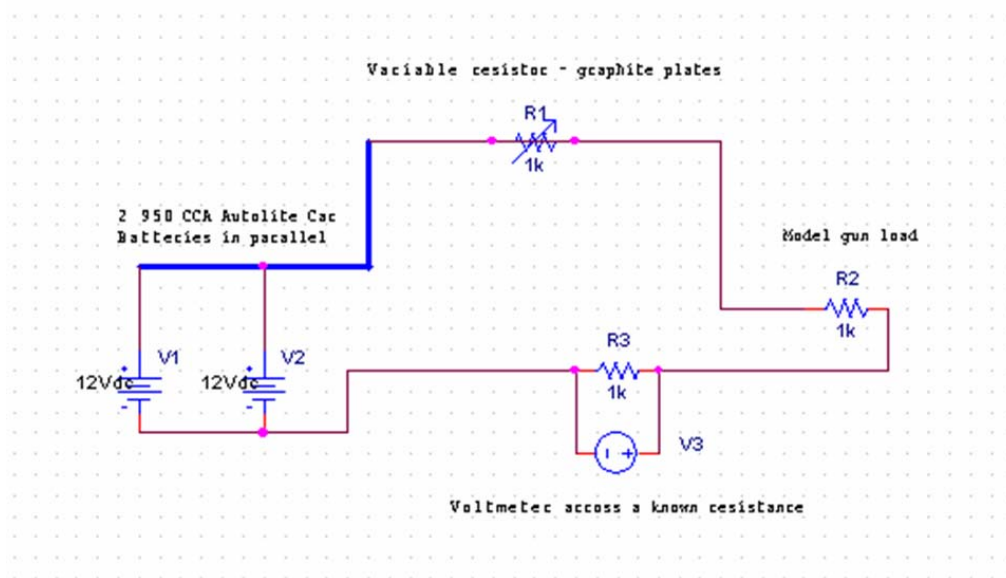


Figure 17. The subtle change here is the removal of the 1kA equivalent fuse. This allowed us to progressively increase the current to a maximum value of 3400A.

## **6. “Floating” the Rails**

After we had selected a power supply (the Autolite batteries), a power coupling mechanism (the eutectic), rail materials (the copper bar stock), a current limiting variable resistor (the graphite plate system), a system for measuring force (the load cells), and a mechanism for recording the temperature rise (the IR camera), we needed to begin integrating the various design elements into a total system. However, we still had not fully addressed the issue of mechanically isolating the gun and armature from the rest of the system. The gun was mechanically isolated from the power supply by use of the eutectic pool, but we had not determined an appropriate means of reducing the forces on the rails so that we could to isolate and record recoil.

My initial inclination was to suspend the system as a pendulum, so that only the restoring force of the pendulum system must be overcome to register a value on the load cells. This force was determined by the mass of the system, the length of the rails, the number of the strings, and the length of the strings, and we could easily determine the size of this correction. Nevertheless we pursued alternative options as we continued to try and make this experiment as unambiguous as possible.

The first alternate to the pendulum system was the notion of floating the rails on dry ice “pucks.” We performed some basic calculations and determined that the force of the static friction would likely be very small, but repeatability was very seriously compromised. Not only would the temperature of the laboratory environment need to be carefully controlled, but we would also need to act rather quickly once the testing was in progress.

The second alternative was to try and employ an available air track. In exploring this option we located a 4m-long air track and modified the inlet to accept a 200psi portable air compressor. We then placed aluminum air carts of varying length and mass on the track, charged the compressor bottle, and injected the air into the track nozzle. At a steady inlet pressure of 80psi we could lift a 4in long aluminum cart with a mass of 200g fairly easily. However, as we added additional weight to the cart (simulating the rail supports) we found that the track was not necessarily limited by the inlet pressure, but

rather the maximum flow rate through the 0.9mm diameter holes along the track surface. The result was that the pre-engineered air carts “floated” while an additional mass on the order of grams or tens of grams made the track ineffective. Even if you disregarded the need for a true straight span of aluminum cart stock and considered the entire span of the air track as a lifting surface, the most you could reasonable lift was on the order of two to three pounds. As the copper alone weighed over ten pounds this alternative was clearly unacceptable.

Other discarded alternatives included attaching the rails to a buoyant material (foam) and literally trying to float the rails on a pool of water and coating a glass surface with oil (or other lubricant) so that the coefficient of friction of the sliding rails would be greatly reduced.

## **B. THE PENDULUM SYSTEM**

We ultimately chose to execute my initial idea of suspending the rails from a pendulum system. The height of the ceiling in the lab defined our maximum pendulum length to be just shy of 9.5ft. Maximizing the pendulum length would minimize the force required to move the system, however, we needed to compromise between a convenient working height and a vertical span that would not be too difficult to stiffen.

We chose to erect a structure with a maximum height of 8ft 1.5in (an 8ft long 2-by-4 standing vertically with another 2-by-4 lying horizontally on top of it) with a working surface (a 3/4in thick sheet of plywood) 31 inches off of the floor of the lab. This arrangement enabled a vertical pendulum length of approximately 5ft 7in (Figure 18).

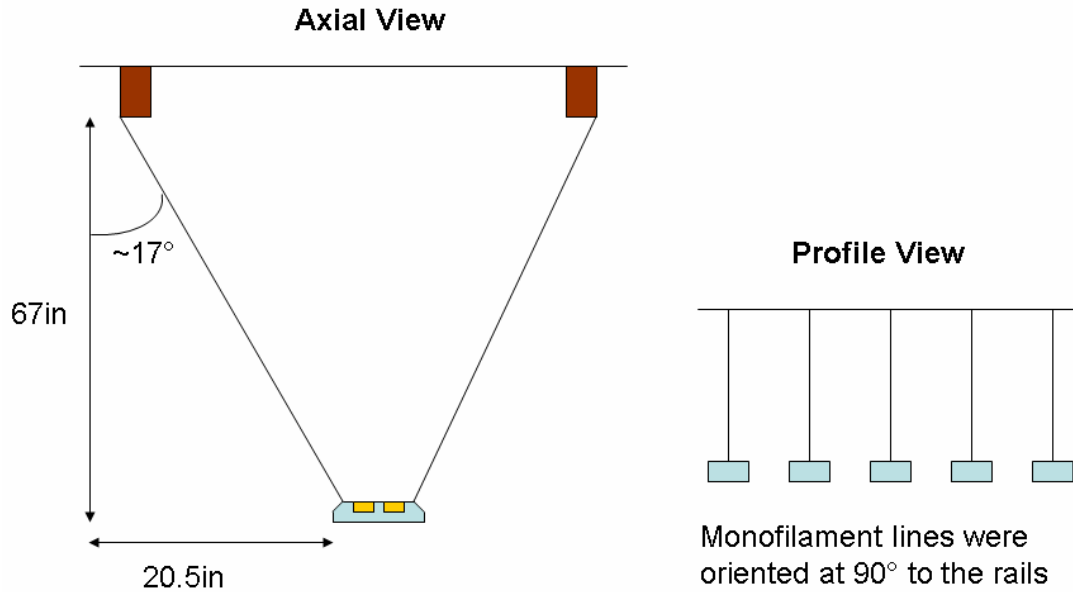


Figure 18. The pendulum system consisted of a series of 5 PVC rail supports suspended by monofilament line. In profile the monofilament was oriented at 90° to the rails, “looking down the barrel of the gun” (i.e. the axial view) you see a small angular deflection (17°) laterally. This deflection greatly enhanced the stability of the system.

The pendulum support structure itself consisted of two 8ft long 2X4” beams separated by 3ft 5in. Since the rails themselves consisted of 6ft long bar stock, we had approximately 2ft of space at one end of the table to place a switching mechanism and the eutectic pools (yet to be designed). In designing the pendulum we anticipated that the rails would be attached to some non-conductive material and this material could be attached to monofilament line and hung from the 2X4” beams.

At this point in the design process it was necessary to manufacture a rail support (or series of supports) that would be light weight, strong, and non-conductive. The key data point in the process was the determination of the expected repulsive force that existed between our two rails.

If two long parallel wires are carrying a current the force of one wire on another can be expressed as a cross product of the current-length and the induced magnetic field.

Since the current-carrying rails in a railgun are in parallel, the length is perpendicular to the induced magnetic field. Thus the force between the rails can be expressed as (Halliday and Resnick):

$$F_{12} = F_{21} = I_1 L B_1 \sin(\theta) = I_1 L B_1 \sin(90^\circ) = \frac{\mu_0 L I^2}{2\pi d} \quad (4)$$

Here F is the force of one wire on another, I is the current, L is the length of the wire,  $\mu_0$  is the free-space permeability, and d is the separation between the wires.

$$F = \frac{\mu_0 L I^2}{2\pi d} = \frac{(4\pi * 10^{-7})(1.862)(4000)^2}{2\pi(2.5 * 10^{-2})} \approx 240N \quad (\text{at } 2.5\text{cm separation})$$

$$F = \frac{\mu_0 L I^2}{2\pi d} = \frac{(4\pi * 10^{-7})(1.862)(4000)^2}{2\pi(5.5 * 10^{-2})} \approx 110N \quad (\text{at } 5.5\text{cm separation})$$

For our nominal design we anticipated a maximum repulsive force of less than 240N (at 4000A) so we determined that available (scrap) polyvinylchloride (PVC) blocks with dimensions of 2in long by 7in wide by 1in deep were sufficient to support the rails. The ultimate design had a slightly different anticipated force (as a consequence of a different rail separation, d) at 110N. Since our rails spanned 6ft we manufactured 6 of the supports anticipating that the copper rod would be sufficiently straight over 1ft spans. Examination of the completed system indicated that only 5 of these supports were necessary, further minimizing the weight.

Each support had a pair of 2.5cm wide by 0.5cm deep slots machined into them on 8cm centers. This corresponded to the orientation of the eutectic pools which were being concurrently designed and manufactured with the switching network.

The upper corners in the long dimension of the support blocks were chamfered at 45 degrees so that a 0.5cm long flat surface was presented for monofilament attachment. This chamfered edge had a bolt hole threaded into its center (width-wise) to accept a nylon bolt (Figure 19).

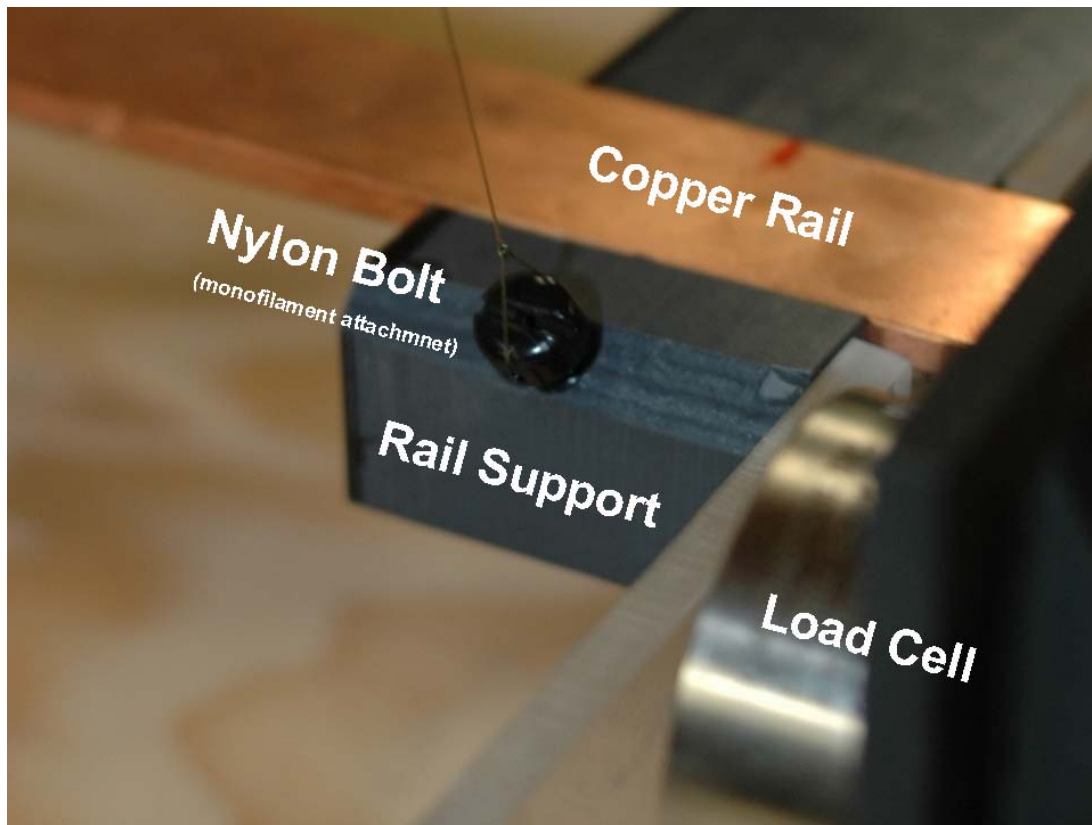


Figure 19. A photo of the PVC rail supports. Near the center of the frame is the threaded nylon bolt and you can just barely discern a hole in the bolt through which the monofilament line is threaded. You can also see a small section of the copper rail that is fit into one of the slots in the PVC rail support.

Once the supports were machined, chamfered, and threaded we placed them equidistant along the span of the rails and using a rubber mallet we pounded the rails into the machined slots. We then drilled one small hole in each of ten nylon bolts, threaded 12ft long monofilament lines into these holes and tied the monofilament off.

After we transferred the rail and rail supports to the working surface of the experiment we threaded the nylon bolts into the bolt holes in the supports and taped the bitter ends of the monofilament lines to the 8ft long beams at the top of the pendulum structure.

Along the outboard vertical surfaces of the 8ft long beams and spaced to match the bolt holes on the rail supports we fastened ten 3in long thread-all rods and threaded

two nuts on each rod (one standard nut and one wing nut). The bitter ends of the monofilament lines were then positioned between the two nuts, and pulled taught as the wing nut was tightened down (effectively squeezing the monofilament line between the nuts and fixing its position, Figure 20). The result was a free-swinging rail and rail-support pendulum system.



Figure 20. The aspect shown here is the chamfered edge of the rail support looking up at the all-thread rod where the monofilament line is squeezed between the two nuts. The advantage of this system allowed for continuous “tweaking” of the pendulum as we sought to have consistent tension on all lines and a square and level presentation of the rails to the eutectic and the load cells.

### **C. THE SWITCH**

The final element of the experimental design, aside from the sensory network, was the switching and eutectic pool module. The basic design consisted of a pair of eutectic pools resting on a pair of copper bus bars that could somehow be repeatedly and rapidly connected or disconnected from the power supply and variable resistor.



We ultimately employed an electrical toggle switch that would engage a pneumatic device which could rapidly open or close a fifty kilo-amp vacuum sealed industrial switch (Meidensha 50kA Vacuum Interrupter S-M101TM). We then cut two 4in wide by 12in long by 0.5in deep copper bus bars and attached the switch to one of these bars. Next we machined a pair of polycarbonate eutectic pools with recessed o-rings as mechanical seals and attached these to the bus bars. We were able fit all of this equipment into a foot-print that occupied less than four square feet so that it could be placed on the working surface without any modifications (Figures 21 and 22).

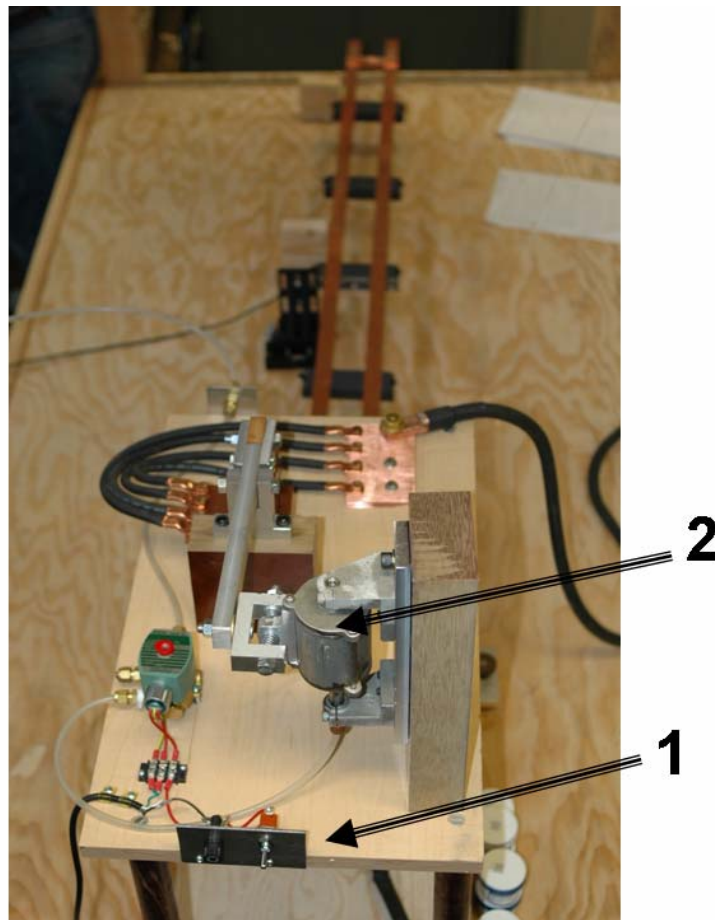


Figure 21. This is an operator's view of the switch – the toggle (1) is centered at the bottom, the pneumatic feed line is on the left, the pneumatic cylinder (2) is on the right, and the upper portion of the 50k Amp switch is attached to the rod coming from the pneumatic device.

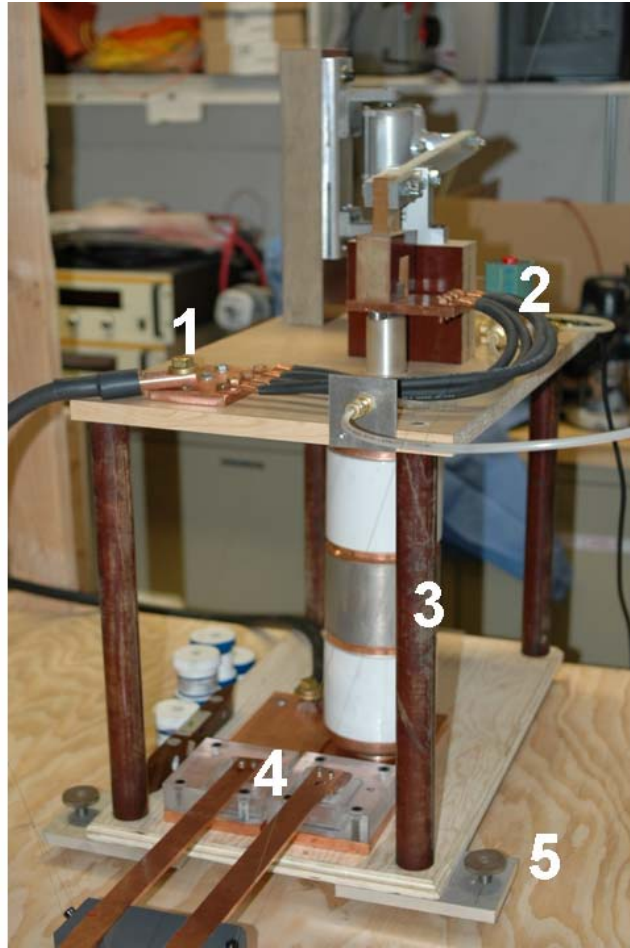


Figure 22. In this view you can see the bus bar (1) from the batteries and variable resistor (upper left) feeding into the top of the mechanical switch (2) via four cables and you can see the large cylindrical switch (3) mounted to the copper bus bar with the eutectic pool mounted to it (4). Also make note of the corners of the lower platform that the switch is mounted on. These “wheel knobs” (5) allowed us to fine-tune the vertical position of the switch (to match the eutectic pool to the lower rail tabs).

#### D. SYSTEM INTEGRATION

With the switch on the table and the eutectic pools coupled to the switch, integrating the free-swinging rails to the eutectic pools was a matter of bolting a pair of 2cm wide by 2cm long by 1cm deep copper tabs to the undersides of the breech end of the rails (Figure 23).

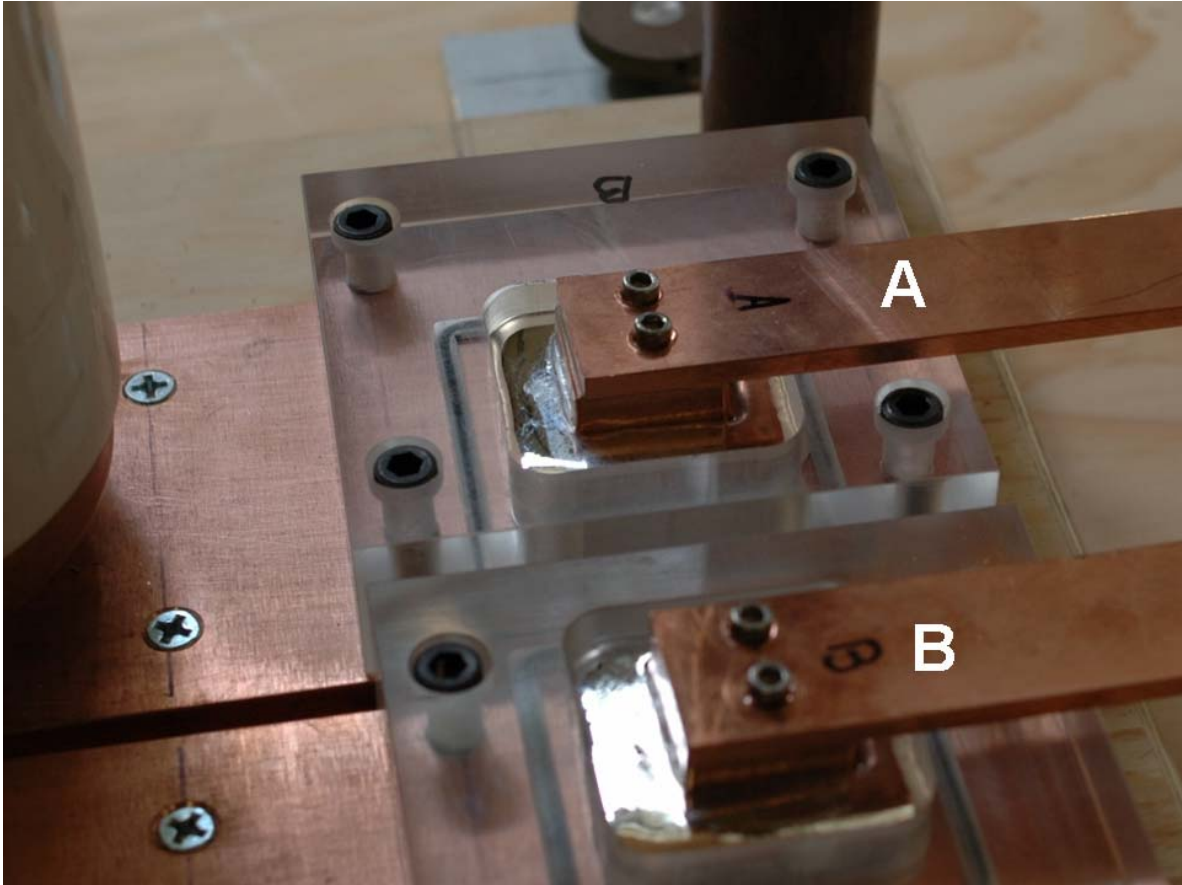


Figure 23. The two rails labeled “A” and “B” were positioned just above the eutectic pools and the fine-tune adjustments on the switch carriage allowed us to raise the eutectic pools to make contact with the copper tabs hanging down from the rails.

Once the pools were filled with eutectic the current path would be (Figure 24) from the positive terminals of the batteries to the variable resistor (1), to the switch (2), to one bus bar into the eutectic pool (3), through the copper tab into the rail (4), across the armature and back down the other rail (5), then through the tab into the eutectic, into the other bus bar, and back into the negative terminals of the batteries (6).

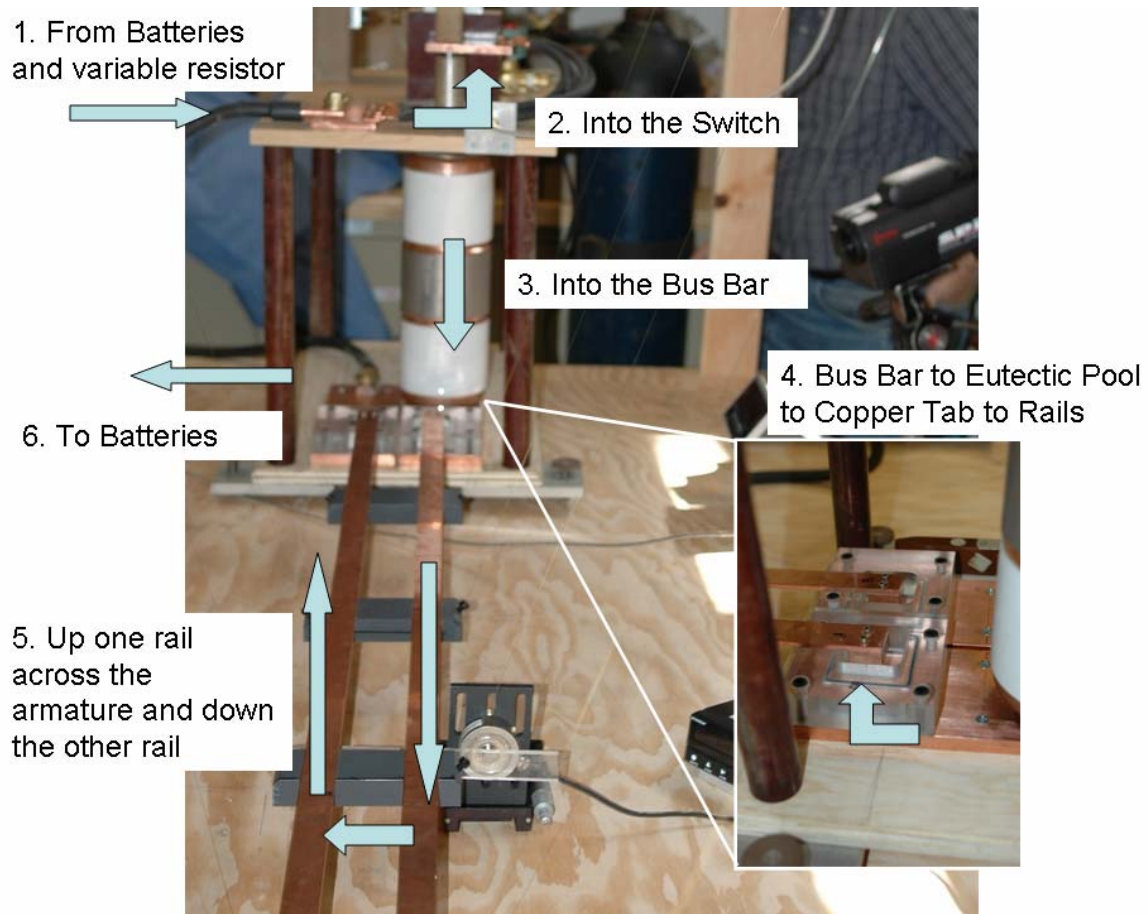


Figure 24. This is the road map of the current path from our batteries through the switching and power coupling network to the rails and back into the batteries.

The tab attached to the undersides of the rails simulated the most-symmetric eutectic test and the “T” bar test in that current was flowing uniformly into a pool of eutectic (from a bus bar) and into a flat, relatively large cross-sectional area of copper.

#### **E. SENSOR INTEGRATION**

Once the pendulum system was fully tested we were ready to begin accessing the capabilities of our sensors and determining proper placement.

The infrared camera was easy to employ. A simple thermocouple check of the ambient conditions and the eutectic temperature was used to calibrate the camera. Then we placed the cross hairs on one of the eutectic pools and selected a sample rate for recording the thermal images (Figure 25).





Figure 25. This picture shows how we recorded the temperature of the eutectic with a thermocouple and calibrated the infrared camera by adjusting the emissivity setting until the temperature shown on the camera matched the temperature on the thermocouple.

At our disposal we also had a newly-acquired high speed camera, a high definition camera, and the usual video recording gear (a JVC camcorder). The high definition camera was to be the wide angle recorder of rail and armature motion, force meter readings, and any other extraneous phenomenon in the experiment (the action of the eutectic, for example). The high speed camera was to be used to record rail motion from a reference point, but we determined it wasn't necessary (the load cells were more than adequate to record rail motion). The usual video recording gear was on standby in case there was other phenomenon that we might want to capture (Figure 26).



Figure 26. This photograph shows how we positioned many of the sensors in this experiment. Going clockwise from our technician on the infra red camera we have the IR camera on a tripod (1), the thermocouple meter (2), micro-strain meter and the load cell on the table (3), the high speed camera on a second tripod (4), the high definition camera on the short tripod (5), the micro-ohm meter on the table (6), and the fluke meter on the battery cart (7). Not pictured are three other load cells, an oscilloscope, and a digital camera for still photos. (The “yellow box” is not part of the experiment – just an out-of-control power cord)

A Keithley 580 Micro-Ohm Meter was used to set the variable resistance in the circuit (at ambient temperature) and a Fluke 87V True RMS Multimeter was used to check the voltage across the battery bus bars. Prior to each experimental trial we verified the resistance and voltage at the cooled ambient condition. After each 3-second current application the resistance was recorded again, and, when possible, the IR camera recorded the temperature rise of the graphite plates.

The last bit of sensory gear we installed was the load cell and force meter. The load cell was attached via machine screws to a micro-adjustment mount. This mount allowed motion fore and aft on the order of micrometers so that we could place the load cell as close as possible to the rail support so that the pendulum would press on the load cell as the switch was closed (if the rails recoiled, Figure 27). With the heavy plywood working surface it was possible to drive wood screws through the micro-adjustment mount and fix the system to the table so that even very high forces on the load cell could be recorded and the load cell would remain in a stationary position. We could very rapidly switch between recording forward motion of the rails (the Lorentz force) and rearward motion of the rails (recoil). The force meter was connected to the experiment via the six-foot-long cable out of the load cell and was placed on the table in a convenient location for monitoring LED output. As a redundant monitoring system we coupled the force meter analog output port to an oscilloscope. Prior to each test we connected the force meter to a laptop computer with the controller software installed so that we could zero the meter and verify the calibration constants.

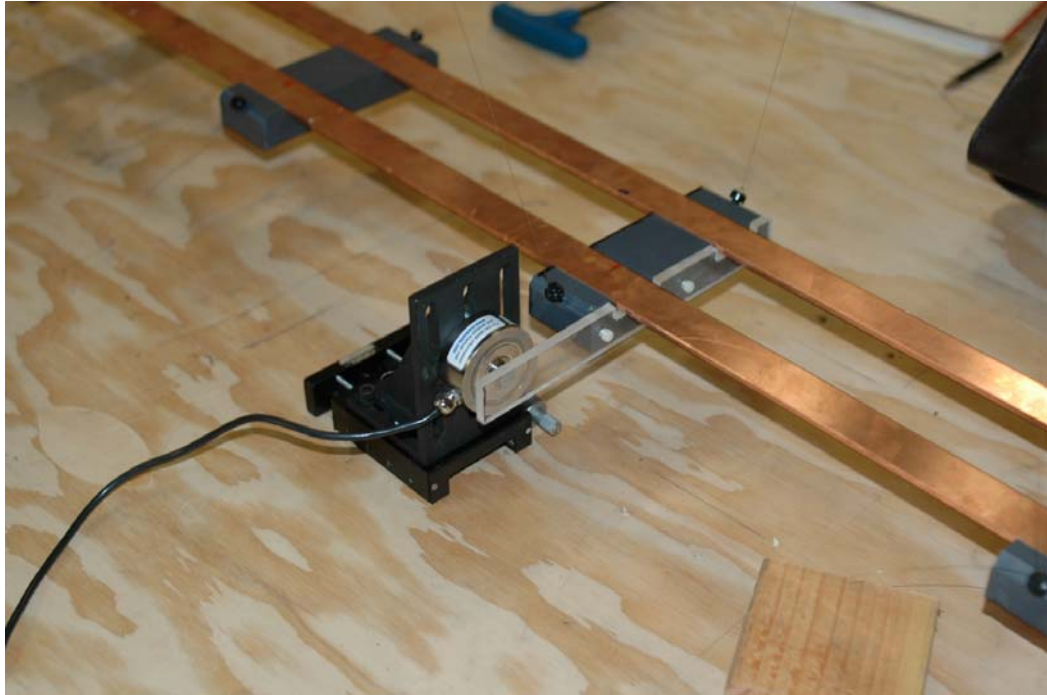


Figure 27. Here you can see the micro-adjustment mount positioned to record the Lorentz force on the pendulum system. The load cell is as close as possible to the arm extending from the rail support without registering a force. In later tests we raised the rails to a height that would allow the load cell to be positioned on the center of the rail support (with no “lever arm” coming off of the support).



### **III. EXPERIMENTATION**

#### **A. EXPERIMENTAL GOALS AND EARLY TRIALS**

As we completed the system integration we arrived at a point where it was time to begin collecting data and determining whether or not our experimental design would adequately represent the aims of this project. In short, we wanted to observe whether or not the pendulum system would effectively isolate the model from the rest of the environment, we wanted to be qualitatively satisfied with the performance of the eutectic, we hoped to record the magnitude of the Lorentz force on an armature fixed to the rails, and we obviously wanted to see if and in what direction the rails would move.

Since the  $L'$  from our nominal design was based upon a rail separation of 2.5cm we had to apply Kerrisk's method again for the 5.5cm separation that was a result of our design process. The new anticipated  $L'$  (via Kerrisk) was  $0.839\mu\text{H/m}$ . Thus the Lorentz force at 1000A on an armature was anticipated to be 0.44N and at 2500A we might expect 2.79N.

As I will describe in the following section we chose to mechanically couple our armature to the rails. Therefore, a factor proportional to, yet less than Kerrisk's  $L'$ , was anticipated to be acting on our system (and recorded via the load cells).

##### **1. Testing the Design**

The trial run of the experiment incorporated an armature which was nothing more than a segment of copper rod stock cut to the dimensions of the rail separation, clamped between two other segments of copper rod stock cut to the dimensions of the outboard edge of the rails (Figures 28-29).

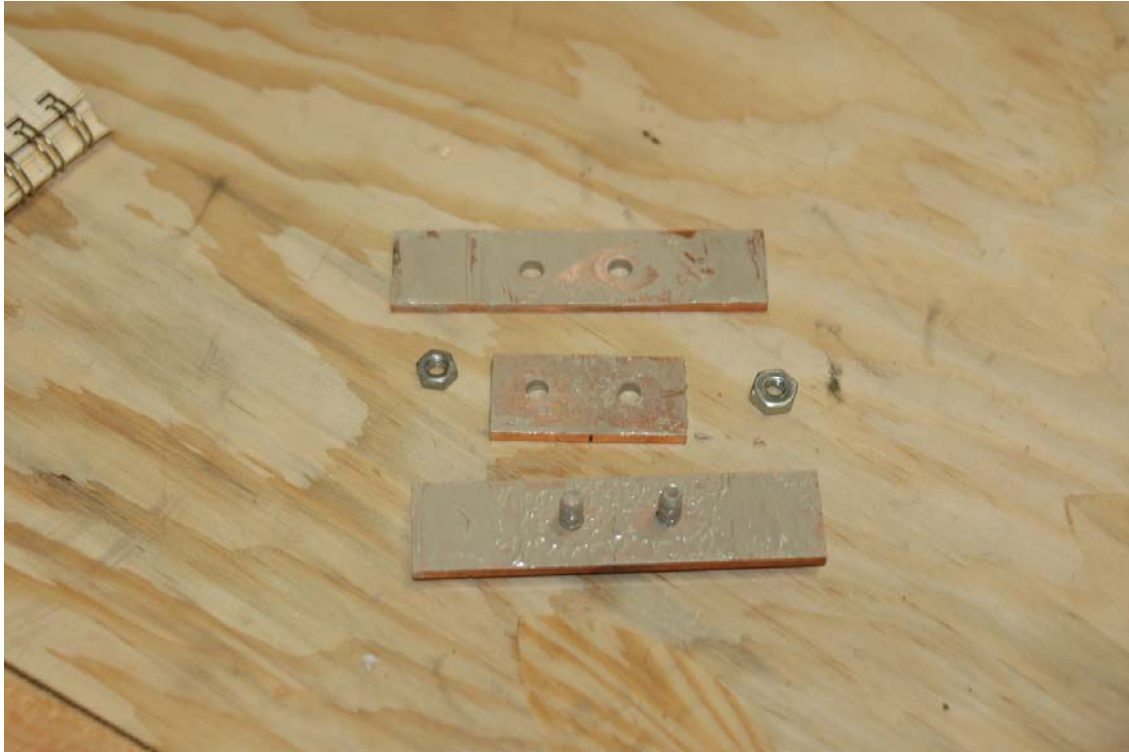


Figure 28. The center segment of the armature was cut to match the rail separation (5.5 cm) and the upper and lower segments were cut to maximum lateral dimension (11.0 cm). The segments were then coated in Conducto-Lube (an organic based silver-paste electrically conductive lubricant) before being bolted together.

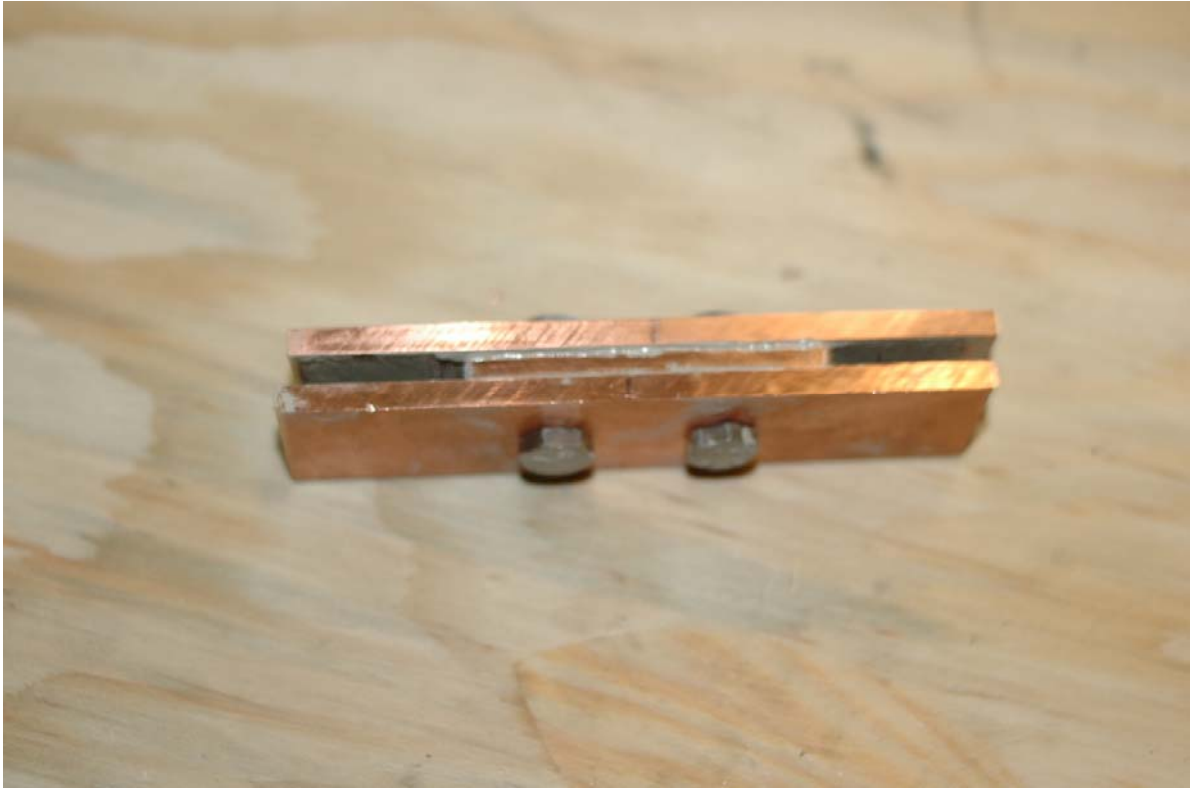


Figure 29. In the assembled armature the torque applied to the bolts varied the ease by which the armature moved along the rails. While we did not record the torque applied, qualitatively, when it was as tight as we could get it (with an eight inch wrench) the armature was effectively fixed in position.

Once the armature was clamped (tightly) opposite of the breech we began adjusting the tension on the monofilament suspension to level the rail pendulum (qualitatively setting uniform tension throughout the system). The monofilament line was elastic so determining uniform tension with the available laboratory equipment was not possible (with any degree of precision), however in future designs monofilament could easily be replaced with stretch-resistant mylar tape or “spider wire” so that it would be possible to set a line tension.

When we were satisfied with the position of the rails we adjusted the switch apparatus to present a level and uniform contact of the breech-end rail tabs to the eutectic pool (this was accomplished with the variable position wheel-bolts on the corners of the lower switch plate, Figure 22). The eutectic pool was filled to a depth of 2cm and the

tabs were wetted to a depth of approximately 0.25cm with the switch in position (providing nearly 0.25cm of clearance between the top of the eutectic pool and the bottom of the rails – see Figures 22 and 23).

With the rail tabs wetted and the switch open we turned our attention to the variable resistor and battery bus network. The consensus in the lab was to begin low and cautiously “ramp-up” the current to no greater than 4000A. Therefore, we decided to connect four of the Autolite batteries in parallel to a common bus bar on the battery cart. As described in the discussion of the experimental design we then connected the positive terminal via a single cable to the variable resistor. The variable resistor was set by selecting an arbitrary number of graphite plates to go between the copper plates and compressing the system while observing the resistance presented by the micro-ohm meter. For the first trial we employed 28 plates and compressed them until we had 15.5m $\Omega$  at ambient temperature (22°C). We then recorded the voltage across the positive and negative battery bus bars with our fluke meter at 12.42V. This procedure set the input current to the switch at the desired 800A. Once the variable resistor was set we connected the resistor via a single cable to the bus bar on the upper plate of the switch apparatus.

The next series of steps addressed our sensors. We began by confirming that the IR camera was set to the appropriate emissivity setting for recording the calibrated temperature rise on the fluid, that an appropriate sample rate was set, and that the cross-hairs were directed at the area of concern (the eutectic pool). We then zeroed the DP-41 force meter via our cross-over connection to a laptop and adjusted an LC305-25 load cell (on the micro-adjustment apparatus) so that a small deflection was recorded on the meter, we then “backed off” the load cell (less than 1 $\mu$ m) until the meter went back to zero. The high definition video camera was set-up to record the motion of the rails and LED output of the meter.

The operation of the experiment employed a two-man team. One individual had the pleasure of toggling the switch and monitoring the temperature rise of the fluid (to terminate the experiment if we were approaching an unsafe condition). The second

individual observed the force meter and general behavior of the rails and/or fluid while recording the change in resistance of our variable resistor before, during, and after the experiment.

## **2. Results of the Initial Test**

As the switch was toggled to apply current to the model gun the system behaved as predicted. With the armature clamped tightly to the rails, the rails and armature deflected away from the breech until the tabs on the rails impacted the edge of the eutectic pool. This displacement showed that at low currents (as low as 400A) the Lorentz force on the assembly was easily measured and therefore the determining the force on the armature should easily be within our capabilities. Unfortunately, in our excitement we had failed to recognize that the sensors were still set-up to record recoil and the rail tabs bottomed-out on the edge of the eutectic pool. When properly positioned one of the rail supports would have pushed against the load cell and all of the force would have been taken up by overcoming the restoring force of the pendulum system and the compression of the load cell.

Rather than delay the experiment further (by repositioning the load cell) we continued to increase the applied current (by further compressing the graphite plates) and observed the behavior of the fluid and the temperature rise in the resistor.

At the conclusion of the trial run we determined that the system was safe and the experiment was repeatable for a range of applied currents from 800A through 3800A. The temperature rise in the fluid was considerably lower than predicted with a maximum of 14°C at an applied of current of 3800A over 3s (Figure 30). This statement does not suggest an upper threshold for applied current; I'm merely stating that conditions were observed to be safe at this level. An item of note is that the thermal rise in the variable resistor seemed to be a greater concern than the thermal rise in the fluid. Our ability to repeat future tests was limited by the time required to cool the resistor.

Another item of note is that there was no arcing throughout the system for this range of applied current.

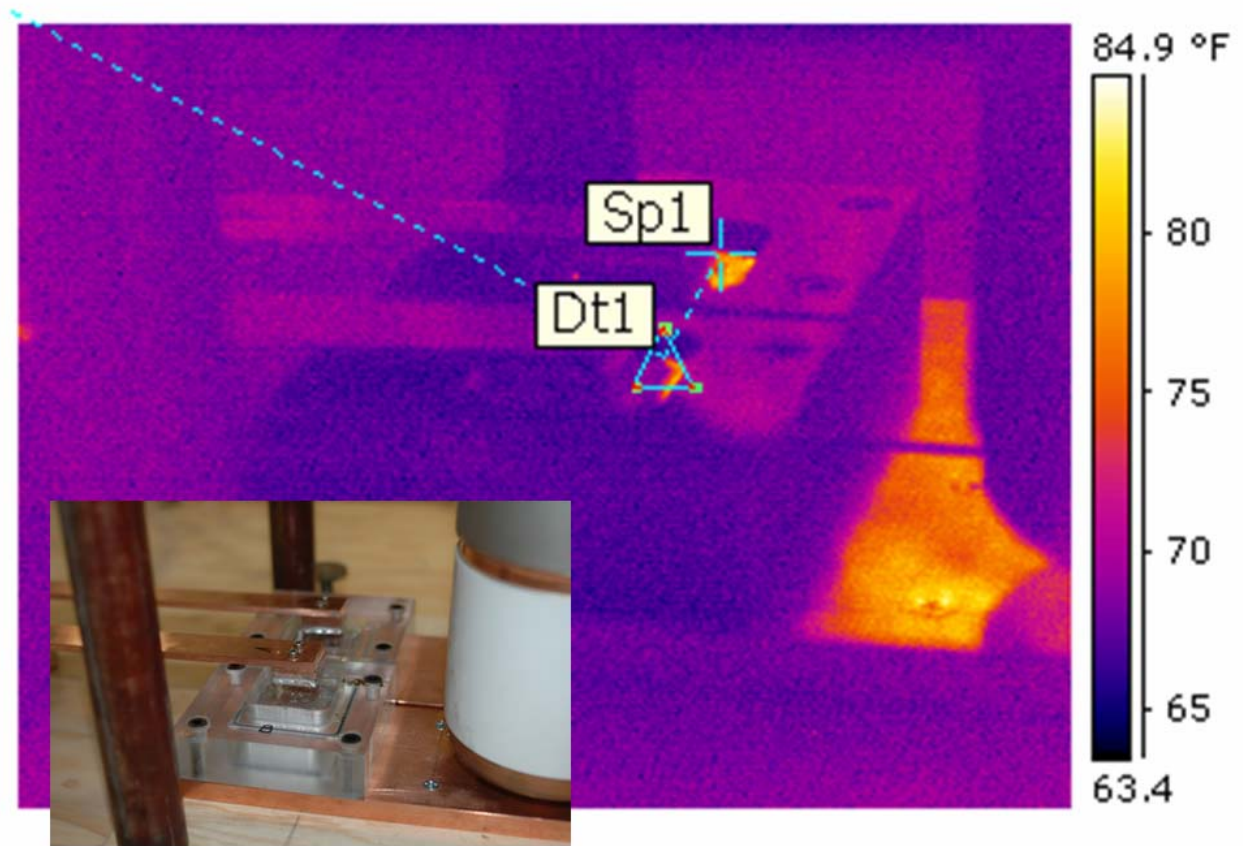


Figure 30. An example of the thermal images we were able to capture during the course of the trial experiment - here you can see calibrated temperature of the fluid and the copper bus bar at 3,800A after 3 seconds. The software processing indicated that the temperature of the fluid was at a maximum of 83°F (28°C) or about 13°F (6°C) above ambient.

## B. CAPTURING THE LORENTZ FORCE

While the resistor was cooling we repositioned the load cell to attempt to capture the Lorentz force on the rail-armature assembly. My hypothesis was that for a fixed mass (rail, armature, and strings) we would have a constant static force that must be overcome before the Lorentz force would be pushing on the load cell. Essentially, whatever force we read on the gauge would be the Lorentz force less some constant. Furthermore, we suspected that the system would behave in accordance with the Lorentz force by increasing with the square of the applied current.

In this second series of tests we sampled the force on the load cells twice for each current setting from 1300A to 3041A (Figures 31 and 32 plot this data). For the entire range of current settings the rail support impacted the load cell while we collected force, thermal, and visual data. The duration between subsequent tests varied (as the thermal rise in the resistor varied with respect to applied current) but we proceeded only when the resistance was stable at close-to-ambient temperatures.

The results of the tests are tabulated below (Table 1). By measuring the voltage across the battery leads (column 1) and the resistance in the system (column 2) we could calculate the applied current at ambient temperature (column 3). The “Force Meter Reading” (column 4) was simply the LED output of our DP-41. The “Force Meter Reading” was adjusted to “Force at Cell” in grams (column 5) by an experimentally derived calibration constant of 0.5747 (174 units on the LED per 100 grams of force). The “Est. Force” (column 6) was the estimated force at the load cell given by the  $I^2$  force dependence equation with the estimated  $L'$  (by Kerrisk). As previously stated the estimated force was expected to be proportional to but greater than the experimental force due to the differences in Kerrisk’s  $L'$  and the constant (call it  $K$ ) describing the electromagnetic character of our system.

Volts	R (m-ohms)	Current (A)	Force Meter Reading	Force at Cell (g)	Est Force (g)
12.49	4.09	3053	279	160	424
12.5	4.11	3041	278	159	421
12.4	5.98	2073	122	70	195
12.4	6.2	2000	110	63	182
12.42	6.61	1878	108	62	160
12.42	6.7	1853	104	59	156
12.4	9.34	1327	60	34	80
12.4	9.38	1321	62	35	79

Table 1. The data collected from this initial system test was done to determine if we could accurately record the Lorentz force acting on the armature. The single data point for the oscilloscope was collected as a “back-up” if the meter (LED) output was variable or unreadable. After the first trial it was evident that the meter was a reliable output. Every 174 “units” on the force meter represented 100 grams-force, thus the meter value divided by 174 and multiplied by 100 converted “units” on the LED to grams-force. This calibration was achieved by using a variety of known loads on the load cells and realizing a linear relationship.

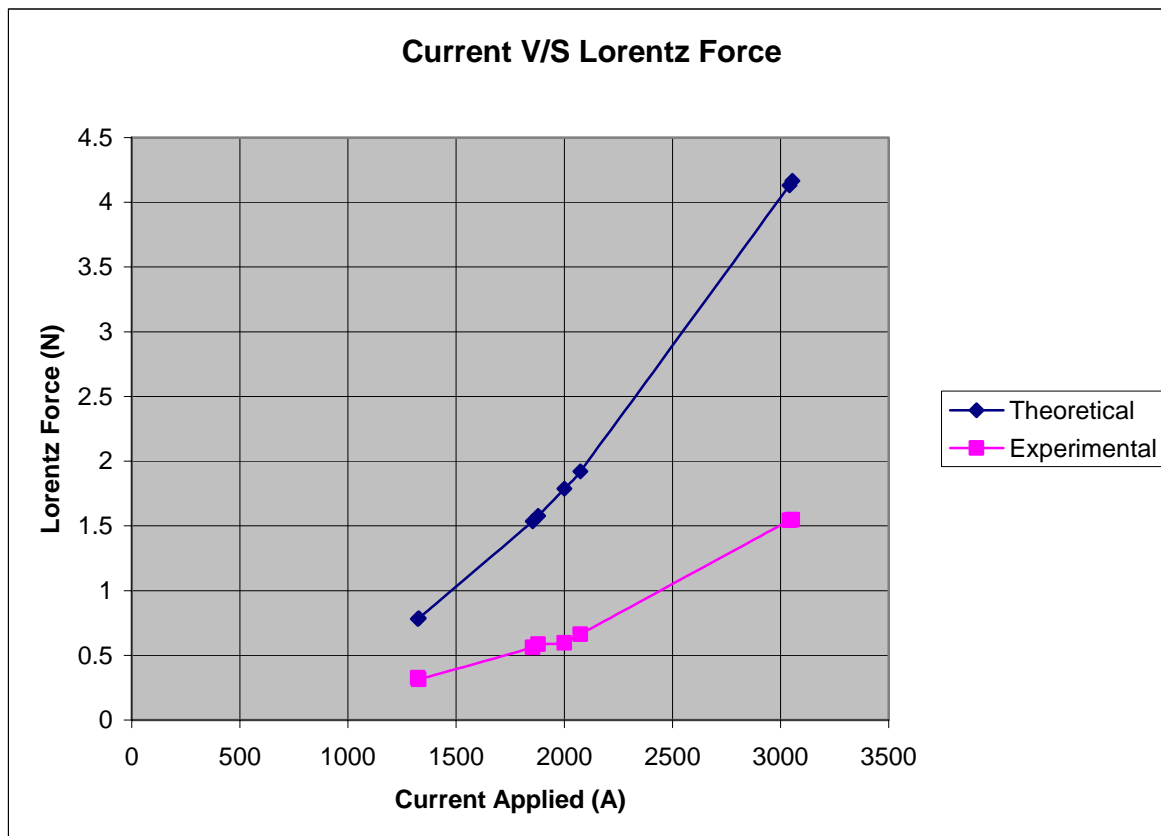


Figure 31. While it may have been beneficial to examine the data set across a wider spectrum of applied currents and a greater number of trials this early series was conducted simply to determine if the system conformed to the Lorentz force equation, where an increase in force goes as  $I^2$ .



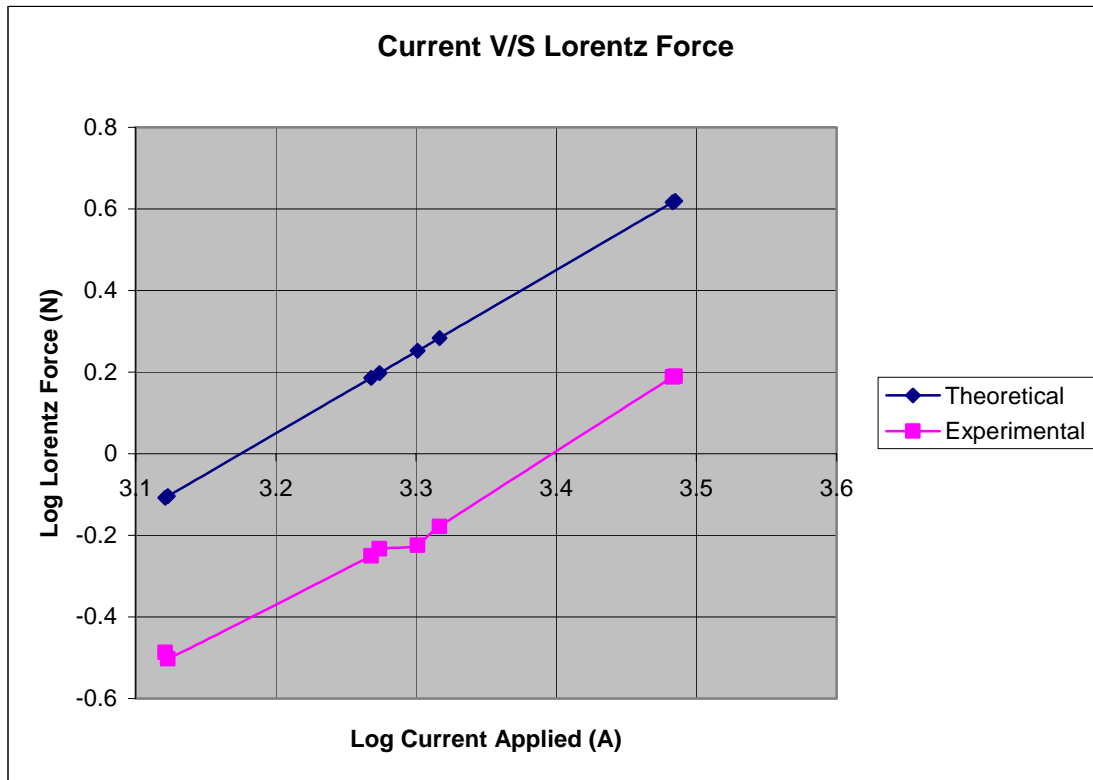


Figure 32. A log-log plot presents an easy visual reference for comparing the experimental data to the  $I^2$  force dependence.

After we collected data on the motion of the entire system it was necessary to determine the value of the constant restoring force of the pendulum. Our estimation of this restoration force was accomplished by “pushing” against the pendulum with a second load cell. In our “push test” we allowed the pendulum to come to rest and zeroed the load cell in contact with the rail support in the usual fashion. We then positioned a second load cell against the rail support nearest to the breech end (opposing the first load cell) and zeroed it. Then, by carefully adjusting the position of the second load cell (via a micro-adjustment device) and pushing against the pendulum we recorded the difference between the first and second load cells and estimated the force required for a given displacement of the pendulum (Figure 33).

"Pushing" Meter Reading – "Fixed" Meter Reading = Restoration Force

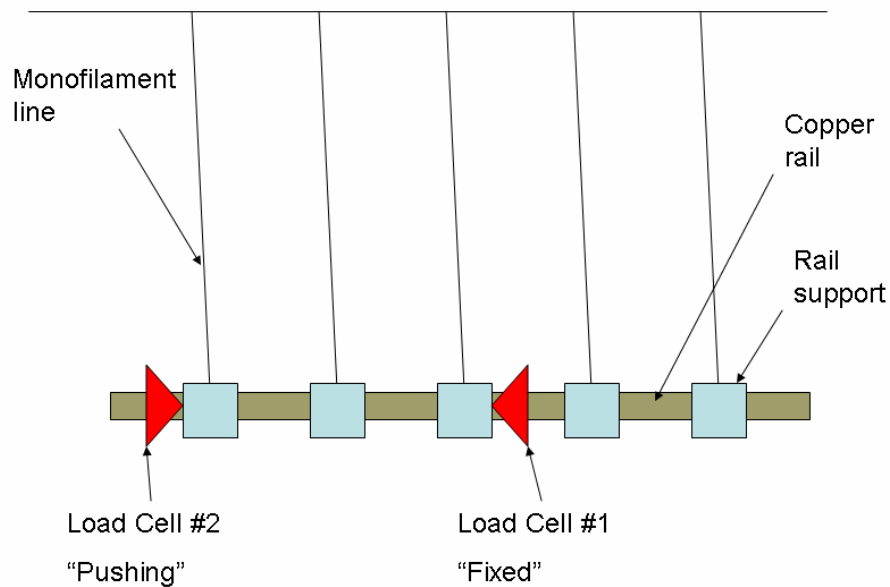


Figure 33. In this simple schematic of the pendulum system you can see how the #1 load cell was fixed in position and zeroed and then the #2 load cell (also zeroed) pushed against the pendulum system.

The force on the fixed load cell (the pendulum deflection) was adjusted to arrive (approximately) at the values of those detected in our experiments to record the Lorentz force. We then subtracted these values from the values of pushing load cell. As anticipated, the force of the pendulum system was effectively constant throughout this range. The restoration force on the system (for this small range of deflections) was estimated to be 2.4gf +/- .2gf (0.024N).

With this last bit of information it was possible to compare our experimental data (for the Lorentz force) with the values calculated using the  $L'$  from Kerrisk. On average the theoretical force was 2.63 times that of the experimental data. By back-calculating a "K" value for the detected force and the applied current of each trial and averaging these values we estimated that the K for our rail-armature system was on the order of 0.33 $\mu$ H/m.

Meter Value	Lorentz Force at Cell (g)	Estimated Force (g)	Kerrisk L' ( $\mu\text{H/m}$ )	K ( $\mu\text{H/m}$ )
278	162	424	0.893	0.334
279	162	421	0.893	0.332
104	72	195	0.893	0.327
108	65	182	0.893	0.331
110	64	160	0.893	0.298
122	62	156	0.893	0.309
62	36	80	0.893	0.373
60	38	79	0.893	0.357

Table 2. The table compares the Lorentz Force recorded at the load cell (experimental data) with the Lorentz force calculated using the L' from Kerrisk. Using the experimental rail-armature Lorentz force and the applied current, I was able to back-calculate a value for "K" describing the electromagnetic character of our system.

In an attempt to fast-forward to a result on the question of whether or not we might observe recoil, we opted to loosen the armature and "see what might happen." With the bolts clamping the segments of the armature loosened sufficiently for the armature to slide with a relatively small application of force we began another series of trials. Reducing the applied current to 800A and "ramping-up," as we had done previously, we found that the entire system was pushing against the load cell once again. While the armature was "free moving" in a sense, it was also very precisely matched to the rail separation such that any asymmetrical motion caused the armature to jam between the rails and act as if it were fixed in place. Furthermore, it is a known fact that current flowing in the same direction on parallel wires tends to cause the wires to attract, thus we expect that some considerable "clamping" of the armature to the rails occurred as current was applied. These factors necessitated a redesign of the armature section if we were going to proceed with attempting to observe recoil.

At this point, the consensus in the lab was that the data from this initial test validated the experimental design - clearing the way to examine in more detail the static force balance of the rail pendulum.

In the performance of these trials we observed a couple items of note. First, the change in temperature of the variable resistor was reflected as an increase of applied

force at the load cell. For each trial the load cell rapidly achieved a sustained force detection (in milliseconds or less) that was constant for at least two seconds. As the applied current caused a temperature rise in the variable resistor, the resistance in the system decreased and resulted in a subsequent rise in applied current. This increase in applied current was detected by the load cells as a steady rise until the switch was opened. Another item of note was the benign behavior of the eutectic. At low current loading the eutectic pool had the usual low frequency ripple with an amplitude on the order of tenths of millimeters. As the current was increased the ripple did appear to increase in frequency a bit, but the amplitude was still very small. This behavior seemed consistent with the favorable results from the “T” bar experiments.

### **C. EXPLORING RECOIL VIA ARMATURE REDESIGN**

Once it was established that this experimental design was valid and precise for measuring the force on the rail and armature system, it was necessary to redesign the armature so that the armature and the rails were mechanically decoupled.

As stated previously, our first attempt at decoupling these objects (loosening the bolts) was a failure. So, we considered various means of lower friction mechanical contact which included rolling projectile, multiple spheres, brushes, and different lubricant and coating systems. However, as these ideas encountered problems it became obvious that a eutectic pool for the armature (similar to the breech-end) was desirable.

A constant concern throughout this process was how to minimize the quantity of the eutectic as we conducted the experiments. Experimentally, the more eutectic we could employ, the lower the current density, and consequently the more benign the behavior of the fluid. The eutectic was rather expensive, so in order to keep the costs down we needed to use as little as possible. Therefore, the first armature redesign employing the eutectic was a simple rectangular eutectic pool with a segment of copper bar stock occupying most of the volume.

We machined a 12cm wide by 4cm long by 1cm deep pool in a polycarbonate block. Then we cut a segment of copper bar stock 4.75cm wide by 4cm long by 1cm deep and centered this segment laterally in the eutectic pool. We then mounted this

polycarbonate block (and eutectic pool) on another micro-adjustment device (which was capable of adjusting the vertical position of the polycarbonate block on a micrometer scale) and filled the voids on either side of the copper segment with eutectic to a depth of 0.5cm (Figures 34 and 35).

The redesign of the armature necessitated a redesign on the bore-end of the rails. We cut a 2.5cm wide by 2.5cm long by 1cm deep segment of copper bar stock, rounded the corners on a belt sander, sanded all surfaces smooth, coated the common surfaces with the silver paste, and mounted this block (via a pair of threaded holes and bolts) to the underside of the bore-end of the rails.

The armature block was then attached to the table with the voids centered under the new bore-end tabs. The block was then raised to wet these tabs to a depth of approximately 0.25cm. This arrangement was very similar to the breech-end in that there was approximately 0.25cm of clearance on all sides of the tabs and 0.25cm of clearance between the rails and the polycarbonate block (Figure 34).

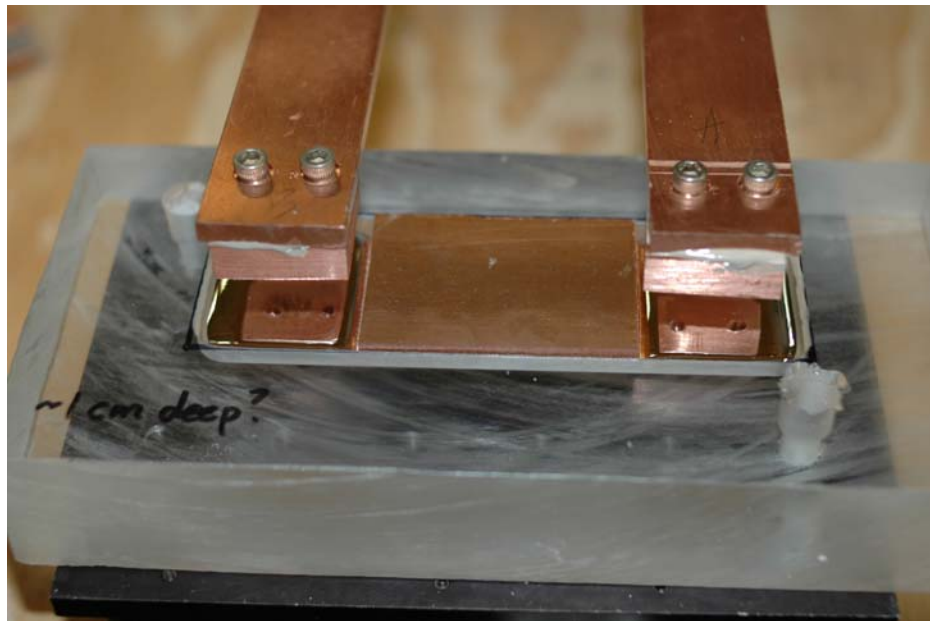


Figure 34. Here you see the polycarbonate pool with a copper bar stock segment centered laterally and the eutectic filling the voids to either side of the segment. Also pictured is the very top of micro-adjustment device (for raising the eutectic pool) and the newly attached copper tabs on the underside of the rail ends. In the first such arrangement the bar stock was 4.75 cm in width in a later trial it was trimmed to 4.25 cm in width (pictured here).

As per the initial experimental set-up we adjusted the tension on the monofilament lines, leveled the rails, set the variable resistance to deliver 1000A, configured all of the sensory equipment, and connected the battery bus to the resistor and the resistor to the switch. The sensory equipment was set-up to attempt to record rail recoil in the usual manner - the high definition camera was positioned to record the load cell meter value and record relative motion of the rails to some reference point (defined on the working surface), the meter was zeroed via the laptop, and the load cell was positioned aft of one of the rail supports and backed-off once the meter registered a deflection.

Once the switch was toggled and the current was shorted across the system we noticed two phenomenon immediately – there was arcing between the rails and the fluid causing the fluid to splatter and the rails did not recoil. After approximately 2 seconds the switch was opened and a one milliohm decrease in resistance was recorded.

When the eutectic splattered, some amount of the fluid left the pool and was deposited on the surface of the polycarbonate. A convenient means of moving the fluid (discovered early on in these proceedings) was to scrape it with a credit card. Once we scraped the fluid back into the eutectic pool and re-centered the armature section under the rail tabs we repeated this test with the same result (Figure 35).

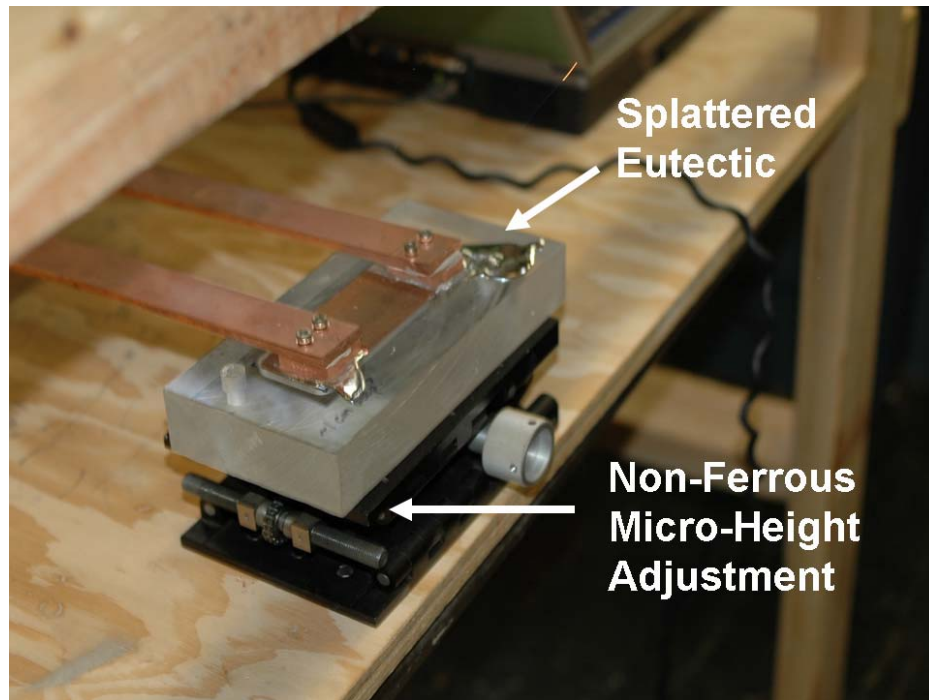


Figure 35. With less than 2 seconds of applied current the arcing between the copper segment and the rail tabs (through the eutectic) deposited a fair amount of the eutectic on the rim of the polycarbonate vessel. This is also a better view of our vertical position micro-adjustor.

In an attempt to decrease the arcing across the fluid (and the subsequent splatter) I removed the copper segment from the eutectic pool and reduced its lateral dimension by approximately one-half of a centimeter, smoothed and rounded the edges, and replaced it in the eutectic pool.

We accomplished one test with this new configuration and noticed significantly less arcing and splatter (arcing began after 2 seconds) and still no discernable rail motion, but were unable to continue the test for two or more seconds due to the erratic behavior of the fluid. While the results were somewhat satisfactory, until we were confident that we would be able to predict the behavior of the fluid we did not feel as though the design had the desired characteristics of being repeatable, predictable, and safe. So, we considered moving forward with this design while paying particular attention to the techniques we had discovered for removing or reducing arcing.

However, before we disassembled the experimental set-up and put the power supply into a safe mode, we opted to remove the copper bar segment from the eutectic pool and attempt to record recoil with an entirely liquid armature. As in previous tests we carefully centered the eutectic under the tabs, adjusted line tension, leveled the rails and set-up our sensory equipment. This time, however, we opted to direct the high definition camera on the action of the eutectic pool with a reference for rail motion based on the relative position of the fixed polycarbonate eutectic pool and the suspended rail tabs. We reconnected the battery, set 1000A as the current limit and shorted this current across the system. This time the model gun behaved like a rail gun and launched approximately half of the liquid armature approximately one foot down range. While this result was not exactly what we had expected or prepared for, again there was no discernable recoil of the rails.

If we were to define the longitudinal axis of the rails as the positive x-direction (with an origin at the breech-end), the lateral axis of the rails as the y-direction (with the mid-point of the rail separation as the origin), and the vertical axis (perpendicular to the working surface) as the positive z-direction, then the displacement from the origin of the rails was only noticed as a slight deflection in the positive z-direction. There was no displacement laterally or longitudinally (in x or y).

#### **D. CONTINUING ARMATURE (RECOIL) TRIALS WITH AND WITHOUT THE COPPER SEGMENT**

As stated in my introduction the most efficient means of advancing this study seemed to be a process of designing, testing, evaluating, and redesigning. The determination that the system was adequate to measure the Lorentz force prompted us to begin investigating techniques to measure recoil. Once we designed and tested various apparatus in an attempt to record recoil, we once again took the time to evaluate the data on-hand and proceed with computer modeling and simulation.

While several armature designs were examined via computer simulations with COMSOL Multi-Physics it became apparent that the time required to design and test a new armature system simply was not available to me. Thus, we made the decision to try



and include ideas for future armature test designs in this write-up, but proceed with the existing design in an effort to quantitatively describe the recoil behavior we had observed to date.

## **1. Further Tests with the Copper Segment**

The next series of tests with the eutectic-pool-and-copper-segment armature was accomplished in the same manner as described in the “Armature Redesign” section above. But, in an attempt to reduce the likelihood of arcing we carefully cleaned and sanded all surfaces of the bore end rail tabs and the copper segment for each trial, and we increased the depth of the eutectic pool to 0.9cm.

While this set-up was not a radical change from the previous experiments we conducted this series with several different goals. First of all we wanted to try and determine if we could find the current threshold below which arcing was not apparent. Secondly, we wanted to carefully observe the eutectic ripple in both the breech end and the bore end and qualitatively describe the action. And thirdly, we were willing to continue to increase the applied current (to 6000A or more) in an effort to locate a threshold beyond which we had indications of recoil.

The experiment began at 400A for 3 seconds and progressively increased by approximately 150A per trial to 1241A before arcing was evident. Throughout this range the eutectic was relatively benign with similar amplitude and frequency of ripple from the breech and bore-end pools and there was no evidence of rail recoil. After 2 seconds at 1241A we observed arcing at the positive rail tab on the bore end. When the copper segment was removed for inspection and cleaning there was some thin deposit of silvery solid (In-Ga) “welded” to the copper segment (on the positive tab side).

Once we cleaned and sanded the copper segment and the rail tabs we reduced the current to 1200A and repeated this trial. After 3 seconds there was no arcing. However, a subsequent trial at 1232A resulted in arcing after approximately 2 seconds. This seemed to indicate that the threshold for arcing of this design was around 1200A.

Over the next 5 trials we increased current from 1250A to 2150A and observed no deflection of the force meter. Through this range arcing was evident and appeared to be more intense as the “fountain” of sparks grew brighter and the damage to the copper segment (absorption of the In-Ga eutectic to the copper) was worse. However, the arcing was only evident along the edge of the copper segment closest to and parallel with the inboard edge of the positive rail tab. Despite placing the copper segment in every possible orientation and varying the size of the eutectic pool on either side of it, there was never arcing on the return path from the armature. While eutectic perturbation was not obviously increasing between subsequent trials, video evidence indicated that both the frequency and amplitude of the ripple was much greater at 2150A than it had been observed at 1200A.

At 2276A we observed our first deflection of the load cell that could possibly indicate recoil. The meter reading at 2276A was 9 (indicating 5gf or 0.049N). With a predetermined pendulum restoration force of 2.4gf (0.0235N), the net force at the load cell can be estimated to have been approximately 7.4gf (0.0726N). During this trial the usual fluid perturbation and strong arcing was evident, so it is impossible to draw any conclusions as to the nature of this force reading, but it was nevertheless a change from the previous trials. Thus we allowed the resistor to cool to ambient temperature and repeated this trial at 2263A. This time the force meter reading showed a peak at 18 which rapidly decayed to 0 then peaked again at 14 and decayed to 0. While there was no discernible evidence in the video recording we have postulated that the rise, decay, and rise was probably due to a sudden impact of the load cell and a bounce, or fluid waves pushing on the rail tabs. There was evidence to support one of these claims from a subsequent trial at 2342A as the meter reading peaked at 6, decayed to 0, and then peaked again at 6 before the switch was opened. However another trial at 2327A had no indication of recoil.

After these series of trials it was necessary to discontinue this portion of the experiment as the eutectic had become thoroughly contaminated and we needed time to analyze the data we had collected (Table 3).

Current (A)	Force Meter Reading After Approximately						Notes
	0.5 sec	1.0 sec	1.5 sec	2.0 sec	2.5 sec	3.0 sec	
813	0	0	0	0	0	0	Nothing
917	0	0	0	0	0	0	Nothing
1005	0	0	0	0	0	0	Nothing
1152	0	0	0	0	0	0	Nothing
1241	0	0	0	0	0	0	Arcing after 3 sec
1325	0	0	0	0	0	0	Arcing throughout
1488	0	0	0	0	0	0	Arcing throughout
1702	0	0	0	0	0	0	Arcing throughout
1896	0	0	0	0	0	0	Arcing throughout
2156	0	0	0	0	0	0	Arcing throughout
2263	18	4	0	14	3	1	Deflection impulses
2276	9	8	0	9	4	0	Deflection impulses
2327	0	0	0	0	0	1	Arcing throughout
2342	6	0	6	0	5	2	Deflection impulses
2344	4	0	6	0	0	0	Deflection Impulses
2332	2	0	0	0	0	0	Liquid Armature
2344	1	0	0	0	0	0	Liquid Armature

Table 3. This table includes all data to date and additional data points from the section entitled “further tests.” Until approximately 1200A there was no arcing at the bore eutectic pool. After approximately 2200A there was some deflection registered on the force meters. However this deflection was “pulsed” indicating a bounce or possible deflection due to fluid motion. The final 2 trials were conducted with a liquid armature, and in each of these trials there was a smaller deflection.

The key conclusion from an analysis of the data is that the theoretical Lorentz force is far greater than the recoil force from the experiment. The average meter value from recoil experiment trials above 2263A in the first 0.5s was 5.71, indicating 3.28gf or 0.032N, while the theoretical Lorentz force at 2263A was 2.29N. The theoretical force on the armature was 76 times that of the average force detected at the load cell. Further tests where we simultaneously measure the recoil and the Lorentz force on a mechanically decoupled armature need to be completed.

## **2. Further Tests without the Copper Segment (All-Liquid Armatures)**

While the first trial of an all-liquid armature was done to simply to satisfy our ever-present curiosity, we determined that further exploration of this set-up would be a good follow-on for the copper segment tests. The rationale was that if the rails were truly recoiling due to the electromagnetic effects and not the rippling fluid or other mechanism, then when the liquid armature was “shot” out of the eutectic pool we would see a similar recoil indication.

Rather than slowly ramping-up the current we opted to continue the analysis of the force balance at or around the “recoil threshold” of 2200A. As in the previous all-liquid trial we simply removed the copper segment from the eutectic pool and brought the fluid level up to some arbitrary depth with the available eutectic (0.5cm in this case). The first trial was at 2332A and unlike the copper segment experiment the duration of the applied current was defined by the action of the armature and not by the action of the switching mechanism. Thus once current was applied some fraction of the eutectic was shot out of the pool (approximately one-third of it) and the circuit was opened. The trial resulted in a force meter deflection of 2 and a rapid decay to 0. Once the eutectic was recovered and the resistor cooled we attempted a second trial at 2344A. This time there was a single meter reading of 1 was observed. Other trials were conducted around this assumed threshold level with similar results (Table 3).

At this point we recovered as much of the eutectic as possible and determined that it was time to begin manufacturing some new armature designs. In an ideal arrangement we would like to collect data on the motion of the rails in positive and negative x-direction simultaneously with the motion of the armature in the positive y-direction. This would allow us to quantitatively compare the two force readings and (Lorentz force on the armature and recoil force) in a single test and definitively make remarks with regards to the force balance (or lack thereof). Possible armature designs which would support this investigation include the use of brush contacts, graphite plates lubricated with silver paste between the rail and armature, a larger pool of eutectic and a lighter material (armature) floating on it, and suspending the armature as a pendulum.

## IV. DISCUSSION

The experimental results of this investigation seem to indicate that we have a valid design for recording at least the Lorentz force on a model railgun assembly and with a little more effort I believe we can use this system to make a convincing argument for supporting or refuting the existence of a reaction force on the rails. Unfortunately it seems as though many aspects of this project could have been stand-alone thesis topics and I lacked the time and resources to effectively tackle every one of them.

What we have accomplished, however, should be the foundation for continued efforts. We have experimentally derived a “K” for our model railgun which is proportional to the theoretical (but smaller than)  $L'$  ( $K=L'/2.63$ ); we have a pendulum system which is effective in isolating the non-conservative forces, we have a very sensitive and robust force measuring system (reliably recording force at 2gf or 0.0196N); and we have established that at least one liquid contact is safe and easy to employ through a range of geometries and currents.

While we were successful at employing the liquid contact to decouple the power supply mechanically from the rails and the rails from the armature, we have not yet tested a system in which we could simultaneously collect data for the force on the armature and the reaction force on the rails. Yet, I believe that once a satisfactory armature design is achieved (potentially an armature-pendulum) we will arrive at a point where we can definitively argue that (at least in this static state) there is little or no reaction force on the rails (little or no recoil).

The Lorentz force experiments were a success. We used nominal values to select materials which would detect a Lorentz force on the order of 0.02-40.0N (depending on applied current) and successfully employed those materials to produce a system that would deliver forces in this range. Our design demonstrated this force in a sustained static state and these tests were safe and repeatable (for several seconds).

The investigation into the recoil mechanism was not as definitive, but I believe the system is sound. After some effort we were able to determine an upper current

threshold below which our armature design exhibited no arcing or adverse eutectic behavior. Beyond this current threshold (1200A) the erratic behavior of the armature (arcing and splatter) did not permit us to record the reaction force with much precision, but the magnitude of the reaction force was observed to be significantly less than the theoretical force on the armature (by a factor of at least 70).

While this result is quite compelling I believe we need to continue this recoil investigation with a redesigned armature. Once the arcing in the armature is eliminated or reduced we should be able to experiment over a wider range of applied currents and provide a convincing argument for refuting the existence of electromagnetic recoil

## BIBLIOGRAPHY

- Allen, I.E., and Jones, T.V.: "Relativistic recoil and the railgun," J. App. Phys., 1990, 67, p.18-21
- Allen, J. E., "Railgun recoil and relativity" J. Phys. D: Appl. Phys., vol. 20, p 1073, 1987.
- Aspden, H., "The exploding wire phenomenon," Physics Letters, vol. 107A, pp. 238-240, February 1985.
- Boyer, T. H., "Energy and momentum in electromagnetic field for charged particles moving with constant velocities," Am. J. Phys., vol. 39, pp 257-270, March 1971.
- Casserberg, B. R., "Electromagnetic momentum introduced simply," Am. J. Phys., vol. 50, pp 415-416, May 1982.
- Graneau, P. and P. N. Graneau, "Electrodynamic momentum measurements," J. Phys. D: Appl. Phys., vol. 21, p. 1826, 1988.
- Graneau, P., "Amperian recoil and the efficiency of railguns," J., Appl. Phys., 1987.62, pp. 3006-3009.
- Graneau, P., and N. Graneau, "The electromagnetic impulse pendulum and momentum conservation," Nuovo Cimento, vol. 7D, pp. 31-45, 1986.
- Halliday, David, Robert Resnick and Jearl Walker, "Fundamentals of Physics (Parts 1-4)/ Extended (Parts 1-5), Seventh Edition, Wiley, 2005.
- Hsieh, K. T., "A Lagrangian formulation for mechanically, thermally coupled electromagnetic diffusive processes with moving conductors," IEEE Trans. Mag., vol. 31, no. 1, 1995.
- Johansson, Lars, "Longitudinal electrodynamic forces – and their possible technological applications," Master of Science Thesis, Lund Institute of Technology, Lund Sweden, September 1996.
- Kathe, E. L., "Recoil Considerations for Railguns," IEEE Trans. Mag., vol 37, no 1, Part 1, January 2001 Page(s):425 - 430
- Kerrisk, J. F., "Current Distribution and Inductance Calculations for Rail Conductors," Los Alamos, Nov. 1981.
- Kerrisk, J. F., "Current distribution and inductance calculations for rail-gun conductors," Report No. LA-9092-Ms, Los Alamos National Laboratory, November 1981.

- Löffler, M., "Recoil forces in electromagnetic accelerators—A short review," in Proc. 4th Euro. Symp. Electromagn. Launch Technol., Celle, Germany, May 1993.
- Maier, William B. II, "Selected Topics in Railgun Technology" (revised 30 July 2007) and various lecture notes and discussions, The United States Naval Postgraduate School, Monterey, CA, 2007.
- Marshall, R. A., and L. C. Woods, "Comment: Origin, location, magnitude and consequences of recoil in the plasma armature railgun," Inst. Elect. Eng. Proc. Sci. Meas. Technol., vol. 144, pp. 49–51, 1997.
- Moon, F. C., *Magneto Solid Mechanics*. New York: John Wiley and Sons, 1984.
- Moyssides, P. G., "Pendulum Experiments and the Fundamental Laws of Electrodynamics," Inst. Elect. Eng. Proc. Sci. Meas. Technol. vol. 35, No. 2, March 1999.
- Parker, J.V., "Why plasma armature railguns don't work (and what can be done about it)," IEEE Trans. Magn., 1989, W. pp. 418-424.
- Pollack, M. and L. W. Matsch, "Electric gun and power source," Armour Research Foundation Report No. 3, Project 15-391E, 1 May 1947.
- Robson, A. E., and J. D. Sethian, "Railgun recoil, ampere tension, and the laws of electrodynamics," Am. J. Phys., vol. 60, pp 1111-1117, December 1992.
- Scanio, J. J. G., "Conservation of momentum in electrodynamics - an example," Am. J. Phys., vol. 43, pp 258-260, March 1975.
- Spann, M. L., et al., "Rapid Fire, Compulsator-Driven Railgun System," presented at The 3rd Symposium on Electromagnetic Launch Technology, April 20-24, 1986, Austin, TX.
- Ternan, J. G., "Equivalence of the Lorentz and Ampere force laws in magnetostatics," J. Appl. Phys., vol. 57, pp 1743-1745
- Weldon, W., M. Driga, H. Woodson, Recoil in Electromagnetic Railguns, IEEE Trans vol 22 no. 6, pages: 1808-1811, November 1986.
- Wesley, J. P., "On Peoglos' measurement of the force on a portion of a current loop due to the remainder of the loop," J. Phys. D: Appl. Phys., vol. 22, pp 849-850, 1989.
- Witalis, E. A., "Origin, location, magnitude and consequences of recoil in the plasma armature railgun," Inst. Elect. Eng. Proc. Sci. Meas. Technol., vol. 142, pp. 197–200, 1995.



Witalis, E. A., and Gunnarson, P.: "Hall effect degradation of rail gun performance," IEEE Trans. Vol 29, pp. 883-888.

Witalis, E. A.: 'The Hall effect magnetohydrodynamics (HMHD) plasma theory with applications'. Proceedings of the 6th MEGAGAUSS International Conference, Albuquerque, NM, November 1992.

THIS PAGE INTENTIONALLY LEFT BLANK

## INITIAL DISTRIBUTION LIST

1. Defense Technical Information Center  
Ft. Belvoir, Virginia
2. Dudley Knox Library  
Naval Postgraduate School  
Monterey, California
3. William B. Maier II  
Physics Department  
Code PHMW  
Naval Postgraduate School  
Monterey, California
4. Railgun Research Group  
Physics Department  
Code PH  
Naval Postgraduate School  
Monterey, California
5. CAPT David Kiel  
PMS 405  
Naval Sea Systems Command  
Washington Navy Yard  
Washington, DC
6. Dr. Roger McGinnis  
PMS 405  
Naval Sea Systems Command  
Washington Navy Yard  
Washington, DC
7. Gene Nolting  
PMS 405  
Naval Sea Systems Command  
Washington Navy Yard  
Washington, DC
8. Fred Beach  
Institute of Advanced Technology  
University of Texas at Austin  
Austin, Texas

9. Dr. Elizabeth D'Andrea  
Director, Swampworks  
Office of Naval Research  
Arlington, Virginia
10. Bob Turman  
Sandia National Laboratories, New Mexico  
Albuquerque, New Mexico
11. Stephen Bayne  
US Army Research Laboratory  
Adelphi, Maryland
12. Ian McNab  
Institute of Advanced Technology  
University of Texas at Austin  
Austin, Texas
13. Roger Ellis  
Naval Sea Systems Command, Dahlgren  
Dahlgren, Virginia
14. Matthew Cilli  
ARDEC  
Picatinny Arsenal  
Picatinny, New Jersey
15. Edward Schmidt  
ARDEC  
Aberdeen Proving Ground  
Aberdeen, Maryland
16. D. S. Sorenson  
Los Alamos National Laboratory  
Los Alamos New Mexico
17. Jack Bernardus  
NSWC, Dahlgren  
Dahlgren, Virginia.
18. James Luscombe  
Physics Department Chair  
Naval Postgraduate School  
Monterey, California

19. Prof. Hans Mark  
Institute for Advanced Technology  
Austin, Texas
20. Rear Admral Clarke Orzalli  
U.S. Navy  
Commander, MARMC  
Norfolk, Virginia